CZECH TECHNICAL UNIVERSITY IN PRAGUE

Faculty of Nuclear Sciences and Physical Engineering

Department of Physics

Research task

Preparation for a measurement of jets with various radii at the ATLAS experiment

Ota Zaplatílek

Supervisor: Mgr. Marek Taševský, Ph.D.

Prague, 2017

ČESKÉ VYSOKÉ UČENÍ TECHNICKÉ
V PRAZE
Fakulta Jaderná a Fyzikálně Inženýrská
Katedra Fyziky

Výzkumný úkol

Příprava na měření jetů s různými poloměry v experimentu ATLAS

Ota Zaplatílek

Supervisor: Mgr. Marek Taševský Ph.D

Consultant: Mgr. Jiří Hejbal Ph.D, Mgr. Roman Lysák Ph.D

Praha, 2017

Prohlášení:

Prohlašuji, že jsem svůj výzkumný úkol vypracoval samostatně a použil jsem pouze podklady (literaturu, software, atd.) uvedené v přiloženém seznamu.

Nemám závažný důvod proti užití tohoto školního díla ve smyslu 60 Zákona .121/2000 Sb., o právu autorském, o právech souvisejících s právem autorským a o změně některých zákonu (autorský zákon).

V Praze 29.1. 2017

ČESKÉ VYSOKÉ UČENÍ TECHNICKÉ V PRAZE
FAKULTA JADERNÁ A FYZIKÁLNĚ INŽENÝRSKÁ
PRAHA 1 - STARÉ MĚSTO, BŘEHOVÁ 7 - PSČ 115 19

Katedra: fyziky **Akademický rok:** 2015/2016

VÝZKUMNÝ ÚKOL

Posluchač: Bc. Ota Zaplatílek

Obor: Experimentální jaderná a částicová fyzika

Vedoucí úkolu: Mgr. Marek Taševský, PhD., Fyzikální ústav, AV ČR, v.v.i.

Název úkolu (česky/anglicky): **Příprava na měření jetů s různými poloměry v experimentu ATLAS / Preparation for a measurement of jets with various radii at the ATLAS experiment**

Pokyny pro vypracování:

1. Prohloubit si teoretické znalosti o jetech s důrazem na použití jetů s velkými poloměry při hledání procesů Nové Fyziky.
2. Seznámit se s několika publikovanými pracemi experimentu ATLAS založenými na hledání Nové Fyziky pomocí jetů s velkými poloměry.
3. Seznámit se s interními technickými články ATLAS na téma použití jetů s malými a s velkými poloměry.
4. Vyjasnit si základní pojmy z této oblasti, tedy re-clustering, grooming, trimming and close-by effects.
5. Seznámit se se softwarovým rámcem v kolaboraci ATLAS pro práci s jety o různých poloměrech a zapojit se do aktivit české skupiny v pracovní skupině JetEtmiss v experimentu ATLAS.
6. Seznámit se s výpočetním systémem GRID a aktivně jej používat.

Součástí zadání výzkumného úkolu je jeho uložení na webové stránky katedry fyziky.

Literatura:

[1] G. P. Salam, Towards Jetography, Eur. Phys. J. C67 (2010) 637.

[2] ATLAS Collaboration, G. Aad et al., Search for massive supersymmetric particles decaying to many jets using the ATLAS detector in pp collisions at sqrt(s) = 8 TeV, arXiv:1502.05686 [hep-ex].

[3] ATLAS Collaboration, G. Aad et al., Search for new phenomena in final states with large jet multiplicities and missing transverse momentum at sqrt(s) = 8 TeV proton-proton collisions using the ATLAS experiment, JHEP 1310 (2013) 130, arXiv:1308.1841 [hep-ex].

[4] R. Camacho et al., Jet Re-clustering in ATLAS, Tech. Rep. ATL-COM-PHYS-2014-1117, CERN, Geneva, Sep, 2014.

[5] T. Javurek et al., The Modeling of the Jet Response for Mass and pT in the Presence of Additional Close-by Jets, ATL-COM-PHYS-2015-574.

Datum zadání: 12.03.2016

Datum odevzdání: 31.01.2017

....

vedoucí katedry

Title:
Preparation for a measurement of jets with various radii at the ATLAS experiment

Author: Ota Zaplatílek

Specialization: Experimental nuclear and particle physics

Sort of project: Research task

Supervisor: Mgr. Marek Taševský Ph.D

Abstract: Actual methods of searching for new physics do not suffice with regular jet algorithms, because the separation of decaying products of a heavy boosted object becomes smaller than a jet with a common radius. Therefore, new techniques are developed. Several of these techniques are described in this thesis. Moreover, topology of such events contains high multiplicity of jets, which can complicate the analysis itself. Most of common applied calibrations were designed for well separated objects and it is not completely verified that it is safe to to apply them in multi-jet events. Potential danger may occur because of very close jets. The answer could be provided by following study of close-by jets. The thesis performs study of close-by effects of jets in mutijet events. The close-by effects were studied using ATLAS data collected during 2015 period. For comparisons with data, Monte Carlo samples of events generated by Pythia 8 were used. The analysis quantifies the close-by effects using balance techniques and invariant balance variables like p_t-balance or response R variables. The close-by-effects are defined using balance variables and are studied as a function of a closeness and jet p_t. The closeness of jets is defined by various distance variables.

The analysis was done using three types of anti-k_t jet with radii $R = 0.2/0.4/1.0$ and two ways of jet construction. Small ($R = 0.2$) and Standard ($R = 0.4$) jets were built from calorimeter's clusters, while Large ($R = 1.0$) jets were constructed by re-clustering procedure from Small ($R = 0.2$) jets. Since re-clustered Large R jets were used, the analysis could also answer, if it is safe to use re-clustering procedure on Small ($R = 0.2$) jets, because of the danger of close-by-effects desribed above.

Key words: anti-k_t jets, radius R of jets, close-by effects, multijet events

Název práce:
Příprava na měření jetů s různými poloměry v experimentu ATLAS

Autor: Ota Zaplatílek

Abstrakt: Současné metody pro hledání nové fyziky si nevystačí s běžnými jetovými algoritmy, neboť např. úhlové rozlišení jetů vznikajících při rozpadu *heavy boodted* částic, se stává nedostatečné. Proto a z řady dalších důvodů se vyvíjejí nové techniky pro hledání nové fyziky. Řada těchto technik je zde popsána. Mimo jiné je nezbytné pro hledání nové fyziky vyvinout vhodné metody pro analýzu již tak problematických multijetových eventů. Při rekonstrukci mutijetových eventů se často používají kalibrace, které byly zkonstruovány pro procesy s dostatečně rozlišenými objekty, nicméně doposud nebylo bezprostředně prokázáno, že je bezpečné použít ony kalibrace i na multijetové systémy. Odpověď by mohla poskytnout analýza věnující se tzv. close-by efektům v multijetových eventech. Právě těmto close-by efektům se věnuje tato práce, která používá data naměřená experimentem ATLAS během roku 2015. Pro srovnání dat byl použit Monte-Carlo generator Pythia 8. Uvedená analýza close-by efektů je založena na tzv. balančních technikách (balance techniques) a zachovávajících se balančních veličinách, jako je např. p_t-balance, nebo response R. Povětšinou byla studována závislost zvolené balanční proměnné na jisté metrice, popisující vzájemnou vzdálenost nejbližších jetů, a příčné hybnosti vedoucího jetu. Pro popis vzájemných vzdálenosti jetů v prostoru byly použity různé metriky např. ΔR, f_{cl1}, f_{cl2}. Uvedená analýza byla provedena pro tři různé sady anti-k_t jetů s poloměry $R = 0.2/0.4/1.0$. Také se zvolily různé způsoby rekonstrukce jetů. Malé ($R = 0.2$) a Standardní ($R = 0.4$) jety by rekonstruovány přímo z kalorimetrických věží, zatímco Velké ($R = 1.0$) jety byly získány procedurou označovanou jako tzv. re-clustering, krerá re-klastruje Malé ($R = 0.2$) kalibrované jety na Velké ($R = 1.0$) již zkalibrované jety. Proto tato analýza může navíc rozhodnout, zda je opravdu vhodné a bezpečné použít $R = 0.2$ jety jako vstup pro re-clustering.

Klíčová slova: anti-k_t jet, poloměr jetu R, close-by efekty, multijetové eventy

Acknowledgement

I would like to express my gratitude to all people who supported me and gave me an opportunity to complete this thesis. My profound thanks go to my supervisor Marek Taševský for his willingness, patience and understanding. I would ĺike to thank to my consultants Roman Lysák and Jiří Hejbal for their technical support and the introduction to World Wide LHC Computing Grid. And finally my gratitudes go also to Martin Dudr for English text corrections.

Contents

Chapter 1

Jets and Jets substructure

1.1 Motivation for large R jet study

Contemporary hadrons colliders designed for the study of high energy physics produce numbers of highly collimated sprays of color-rich particles in the final states. These sprays, so-called jets, are frequently produced as a product of hard partons interactions from (hard scattering) at proton-proton collisions. Jets became necessary tools for description and understanding of experimental particle physics within and beyond the Standard model.

With ambitions to collect more data effectively with increasing luminosity, also the rate of secondary processes grows. Initial state radiation, multiple-parton interactions, underlying events and pile-up became more significant, therefore events, as well as the jets, are affected by them. For illustration, expected contamination from the pile-up at high-luminosity LHC reaches $10-20$ GeV per unit area in (y, ϕ) plane.[1]

For instance standard jet algorithms and techniques for sufficiently boosted decay products of W boson, H boson or top quark start to fail. It starts to fail owning to separation of quarks (as decay products of these boosted topologies). This separation becomes smaller than common radius of jets [2]. Therefore, reconstruction of single massive jets with large radii R (often called fatjets) represents a solution. Accordingly it is substantial to develop effective substructure techniques and ways for finding, reconstruction, tagging of these large R jets.

Jet substructure methods belong to useful techniques for jet analyses. These procedures are helpful to reach more information about inner structure of large R jets. For example, they could determine number of subjeties, distinguish type of initial particle of QCD branching or discriminate secondary process like initial state radiation, multiple pp interactions and pile-up. Consequently, they improve the jet resolutions.

For instance, grooming methods belong to jets substructure. Grooming counts trimming, mass-drop filtering and pruning and the others. The mentioned techniques will be discussed below. For better understanding let's start with a short description of jets construction and basic properties of jets algorithms because grooming are based on them.

1.2 Jets algorithms

So-called jet algorithms serve for finding the jets. They can be one of two kinds: either cone or clustering jets algorithms. Basic ideas of the mentioned algorithms are following: cone algorithms surround significant flows of particles by cones with radius R. Whereas clustering algorithms combine two objects i, j retrospectively. They use this procedure repeatedly, which is based on comparing two distances d_{ij} and d_{iB} to find the leading particle, which stays at the beginning of QCD branching. Variable d_{ij} represents mutual distance of two considered clusters i and j whereas d_{iB} describes jet-beam distance with respect to the main cluster i. The clustering jet algorithms are also designed to comply with collinear and infrared safety conditions in general. These significant properties permit comparison of the data with theoretical calculations instead of the basic type of the cone algorithms.

The most common use of clustering algorithms in hadron-hadron collisions are described by formula (1.1) using kinematic variables: transverse momentum p_t, rapidity y, azimuth angle ϕ and a set of input parameters: jet radius R and a parameter p, which is explained below.

$$d_{min} = \min(d_{ij}, d_{iB}) \quad \text{where} \quad d_{iB} = p_{t_i}^{2p}, \qquad d_{ij} = \min(p_{t_i}^{2p}, p_{t_j}^{2p}) \cdot \frac{\Delta R_{ij}}{R}, \\ \Delta R_{ij} = \sqrt{(y_i - y_j)^2 + (\phi_i - \phi_j)^2} \tag{1.1}$$

The parameter p determines the weight of transverse momentum p_t. It also distinguishes the method for assigning particles to a jet. Accordingly it is possible to differentiate the k_t ($p = 1$), anti-k_t ($p = -1$) and Cambridge/Aachen ($p = 0$) algorithms. The clustering itself is described by followings steps.

1.) determine variables d_{ij} and d_{iB} of all clusters i and j

2.) determine $\min(d_{ij},\, d_{iB})$ of all cluster i and j

  a.) if $d_{ij} = \min(d_{ij},\, d_{iB})$, then:

    I. cluster j is megred with protojet i

    II. count 4-momenta of protojet again according to recombination scheme

  b.) else if $d_{iB} = \min(d_{ij},\, d_{iB})$, then:

    I. denote object i as a jet

    II. remove all merged particles (clusters) form the datalist

3.) repeat the procedure from point 1.) until the list of clusters is empty

Note that the indices i and j generally denote different clusters in every iteration. Therefore clusters (during iterations in a cycle) are assigned to different protojets. In other words, jets are found all at the same time, unlike the case of cone algorithms where jets are found sequentially. Moreover this procedure of merging is infrared unsafe. For example: well separated soft gluon could create a jet, thus another input parameter is necessary. Requirement on minimal transverse momentum of jet $p_{t_{min}}^{jet}$ is used to solve it.

1.2.1 k_t algorithm

The k_t algorithm is described by $p = 1$, hence it clusters soft particles first and hard particle last. That causes an irregular output in the space of rapidity and azimuth angle (y, ϕ), which could complicate reading from special types of detectors and further an application of nonperturbative corrections. This makes the k_t algorithm less suitable for experimental use [4]. Despite of that is k_t algorithm well used for pile-up subtraction methods and procedures for filtering of soft particles like trimming technique.

1.2.2 Cambridge/Aachen algorithm

Cambridge/Aachen algorithm is characterized by $p = 0$ and therefore its clustering formulas are reduced on $d_{ij} < \frac{\Delta R_{ij}}{R}$ and $d_{iB} = 1$. It modifies itself re-clustering condition for merging protojet i and particle j from second point of clustering procedure as follows.

$$\Delta R_{ij} < R \tag{1.2}$$

Unlike k_t or anti-k_t algorithms the Cambrifge/Aachen does not respect the transverse momenta of particles, only their mutual distances. Therefore, Cambridge/Aachen represents a basic algorithm of sequence clustering algorithms.

1.2.3 anti-k_t algorithm

In the case of anti-k_t algorithm is $p = -1$. As a consequence hard particles are clustered first. Parameter $p = -1$ is also related to symmetrical output in $(\phi \times y)$ space and insensitivity to soft particles. Thanks to collinear and infrared safety the anti-k_t algorithm is the most widely used one among all others nowadays [3].

1.3 Angular separation

Any jets algorithm requires a set of input variables. Jets radius R represents the most ordinary of them to characterize volume (respectively size) of jets. Consequently, right choice of radius R is crucial. Angular separation ΔR could be helpful. This dependence ΔR as a function of transverse momentum p_t of decaying particle is shown in fig. 1.1 for decay of boosted Z' boson in following channels: $Z' \to t\bar{t}$, weak decay of top quark $t \to Wb$ and subsequent hadronic decay of W boson to light quarks. Angular separation ΔR has a hyperbolic dependency on transverse momenta p_t of decaying particle with invariant mass m as it is seen in fig. 1.1. For analytic approximation could be derived following formula.

$$\Delta R \approx \frac{2m}{p_t} \tag{1.3}$$

Consequently for jet studies are products after the first decay of heavy boosted objects ($Z' \to t\bar{t}$) close enough. According to fig. 1.1, the separation $\Delta R(W, b)$ between W boson and b quark is approx. 0.4. However the following decay of $W \to q\bar{q}$ provides the angular separation of created quarks pair $\Delta R(q\bar{q})$ in area $0.6 - 1.2$ with respect to the transverse momenta of W boson. The fraction $2m/p_t$ increases, thus large R jets (fatjets) with radii $R \approx 1.0$ are needed. Hence, the research of new heavy mass particles behind the Standard model requires large R jets. [2] [5]

1.4 Grooming

Grooming is used for subtraction of secondary processes and pile-up in large R jets. Further it improves the mass resolution of boosted objects. Jets substructure methods could be used for new physic research. Grooming contains many techniques, nevertheless only the most popular ones will be described, namely Mass-Drop Filtering (often so-called as the filtering), Trimming and Pruning.

1.4.1 Mass-Drop Filtering

The first of presented grooming methods is the Mass-Drop filtering technique which was developed and optimized for the study of Higgs boson decay in $H \to b\bar{b}$ channel [8]. Also it was used for weakly interacting massive particles for dark matter research [7].

Mass-Drop procedure requires two input parameters μ_{frac} and y_{cut}. Parameter μ_{frac} describes maximal mass fraction. Second variable y_{cut} could define energy sharing between two

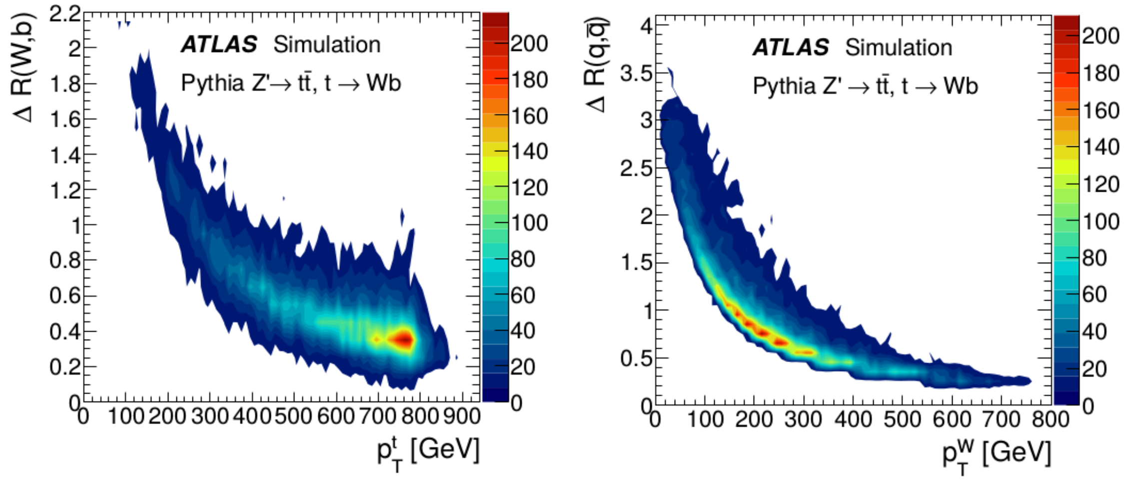

(a) $t \to Wb$ (b) $W \to q\bar{q}$

Figure 1.1: Angular separation ΔR of decaying boosted Z' products and following decay. Fig. (a) is describes process: $t \to Wb$ whereas fig.(b); is associated with $W \to q\bar{q}$ channel. Data are simulated by Pythia. Initial and final state radiation, as well as underlying events are not included. Taken from [2]

subjets in original jet [2], but it also represents minimal relative symmetry, of two Cambrige/Aachen subjets. Since Cambridge/Aachen algorithm clusters the closest particles with small mutual angles first, therefore it was used for suitable symmetry detection.

The Mass-Drop contains two stages. The first one is denoted as Mass-drop and symmetry, whereas the second one is called filtering itself. Both stages are described schematically in fig. 1.2. First stage uses the above mentioned parameters and its analytic description show following formulas eq.(1.4).

$$\frac{m^{j_1}}{m^{jet}} < \mu_{frac} \qquad \text{and} \qquad \frac{min\left[(p_t^{j_1})^2, (p_t^{j_2})^2\right]}{(m^{jet})^2} \times R^2_{j_1,j_2} > y_{cut} \tag{1.4}$$

Where indeces j_1 and j_2 are associated with two considered subjets of original jet. Denoted superscribes are chosen in accordance with mass relation $m^{jet} > m^{j1} > m^{j2}$. The other used variables denote transverse momenta $p_t^{j_1}$, $p_t^{j_2}$ of subjets with their mutual distance $\Delta R_{j_1,j_2}$. Above mentioned incoming parameters μ_{frac}, y_{cut} are used as well. Value of μ_{frac} is chosen at range of tens percents commonly. For instance, parameters $\mu_{frac} = 0.67$ and $y_{cut} = 0.09$ were optimized and used for study of Higgs boson $H \to b\bar{b}$. [2]

If considered jet does not satisfy criteria in eq. (1.4), then jet is discarded. The second stage of algorithm follows - filtering itself. Now, acquired jet is re-clustered by Cambridge/Aachen algorithm with new radius $R_{filt} < R_{j_1,j_2}$. Definig of R_{filt} according to eq.(1.5) was shown as very effective.

$$R_{filt} = min\left[0.3, \Delta R_{j_1,j_2}/2\right] \tag{1.5}$$

All constituens outside the three hardest jets are removed in the end. The choise of three could provide one additional radiation in such two-body decay to be captured. [2, 6]

More understanding of subjets could be achieved using equations eq.(1.4, 1.3) and fig. 1.1. If a $W \to q\bar{q}$ process is assumed with a W boson mass $m^W \approx 80$ GeV and transverse momentum of roughly $p_t^W \approx 200$ GeV (mean value of p_t estimated from fig. 1.1 (b), then the expected separation $\Delta R_{q\bar{q}}$ of quarks according eq.(1.3) will be approximately $\Delta R_{q\bar{q}} \approx 0.8$. Minimal transverse momentum of quark could be estimated using $y_{cut} = 0.09$. It performs $min(p_t^q, p_t^{barq}) \approx 30$ GeV. Consequently, relative transverse momentum of second subjet is $p_t^{j2}/p_t^{jet} > 0.15$.

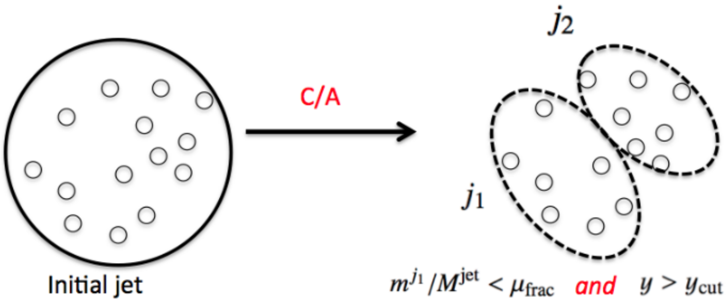

(a) Mass-Drop procedure

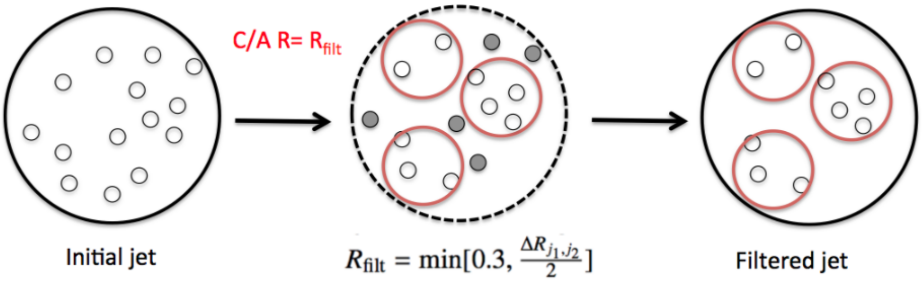

(b) Filtering procedure

Figure 1.2: Schema of jet Mass-drop filtering procedure, taken from [2]

1.4.2 Trimming

Trimming technique uses clustering k_t algorithm ingeniously. Method requires two input parameters: radius R_{sub} and f_{cut} parameter. During this procedure, all constituent particles within radius R jet are clustered again by k_t algorithm to small subjets with different radius R_{sub} ($R_{sub} < R$). Provided that fraction of transverse momentum of i-th subjet $p_{t_i}^{sub}$ with respect to the transverse momentum of jet p_t^{jet} is less than incoming parameter f_{cut} then subjet i is removed from the jet.

$$p_{t_i}^{sub}/p_t^{jet} < f_{cut}$$

Taking into account that k_t-algorithm merges soft particle first, trimming also decreases pile-up, multipartons interaction and initial-state radiation without change of hard components in final states. Typically $30 - 50$ % of mass is lost during the trimming procedure in case of low-mass jets ($m^{jet} < 100$ GeV) of light quarks or gluons. Boosted decaying objects (with the same mass) lose less. [2] Graphical scheme of trimming procedure is seen in fig. 1.3.

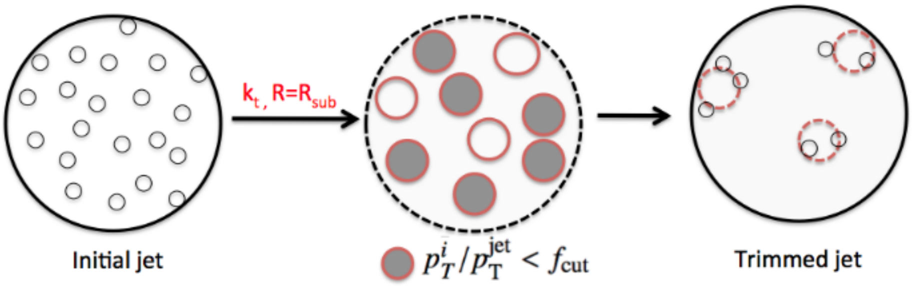

Figure 1.3: Schema of jet trimming procedure, taken from [2]

1.4.3 Pruning

The last described grooming technique is pruning, which also suppresses soft particles with small relative p_t like trimming. In addition, it prohibits wide-angle radiations, too. Pruning procedure requires two incoming parameters R_{cut}, z_{cut} and list of just found anti-k_t or Cambridge/Aachen jets. Meanings of R_{sub} and z_{cut} is explained below. The pruning procedure itself is invoked repeatedly in each step of recombination of two objects by jets clustering algorithm. Consequently, subjets construction is not required. K_t or Cambridge/Aachen algorithms are used for re-clustering ordinarily. Flow scheme of pruning procedure is following.

1. apply k_t or Cambridge/Aachen clustering algorithm on constituents of just found jet

   a.) determinate two values with respect to considered particle j and protojet i:

      I. relative increment of transverse momenta p_t^i/p_t^{i+j}

      II. mutual distance ΔR_{ij}

   b.) evaluate the conditions: $p_t^i/p_t^{i+j} < z_{cut}$ and $\Delta R_{ij} < R_{cut} \times 2m^{jet}/p_t^{jet}$

      I. if one or both conditions are fulfilled then merge i and j

      II. else remove particle j

   c.) continue with procedure from step a.) with another particle j' selected by k_t or Cambridge/Aachen jets algorithm

It is obvious from the flow scheme, that input parameter z_{cut} describes a maximum relative transverse momentum of particle in pruning jets. Choice of this parameter vetoes soft particles. Parameter z_{cut} usually is less than 0.1. Second argument of pruning R_{sub} parameter is applied to limit the angular separation of jet's conctituents, since $2m^{jet}/p_t^{jet}$ represents the angular separation of two prong sujets in the original jet, see eq.(1.3). Value of R_{sub} uses to be in order of tens of percent. [2] Graphical scheme of pruning procedure is shown again in fig. 1.4.

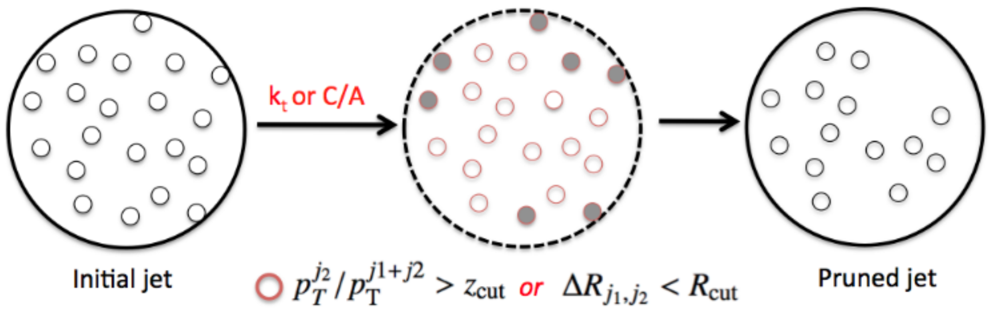

Figure 1.4: Schema of jet pruning procedure, taken from [2]

Chapter 2

The data analysis: Close-by effects of jets

2.1 Motivation for Close-by effects study

Jets as a spray of significant collimated flow of energy could be constructed from various types of objects. Particles, tracks or calorimeter clusters could be used. However, real data have to be corrected back to the so-called truth (particle) level.

Most of the corrections were developed on well-separated objects which occur in dijets or γ+jet events. Nevertheless the reconstruction of different processes (especially those used to search for new physic) possess very different topology to each other. For example decay of boosted scalar and vector bosons like $H \rightarrow b\bar{b}$, $Z \rightarrow b\bar{b}$ or $Z' \rightarrow t\bar{t}$. Such $t\bar{t}$ events count at least 6 jets which could render this process potentially dangerous. Jets may be close enough from one to another to alter their properties. Jet properties could be affected by the change of jet shape or by effective energy sharing between the closest jets. These two phenomena are the consequences of other two phenomena, called energy-flow and color-flow, respectively.

The energy-flow is caused by the energy sharing due to an overlap of jet areas. When the anti-k_t clustering algorithm (the most often used safe algorithm for jet construction [3]) is used it starts to add particles to the hardest one, hence the energy of the leading jet increases, while the energy of the closest jet decreases. So it is an anti-correlated effect with respect two the closest jets.

Further on, in the case of the color-flow, it is assumed that with decreasing mutual distance between two jets also the probability from migration of color-charge particles between two jets increases. This effect is also called the correlated out-of cone deposit of energy. Consequently the jet particle composition is changed, which changes its shape.

Studies of close-by effects have been performed previously in γ+jet and Z+jet events using the anti-k_t $R = 0.4$ jets at $\sqrt{s} = 8$ TeV [9]. This analysis uses collected data in 2015 at a central mass energy $\sqrt{s} = 8$ TeV during pp runs by $ATLAS$ experiment and Monte-Carlo Pythia 8 samples for comparison.

The study is based on the analysis [10]. It uses multijet events and data with higher statistics than the previous study [9]. Therefore, it is able to investigate a larger of phase space. In comparison with the analysis [9] anti-k_t $R = 0.4$ leading jets are used. The recoil system includes anti-k_t $R = 0.2$ (Small), anti-k_t $R = 0.4$ (Standard) or anti-k_t $R = 1.0$ (Large) jets. Small and Standard jets were built from calorimeter clusters directly while Large jets in recoil system were obtained by re-clustering of anti-kt Small ($R = 0.2$) jets. Consequently, calibrations and uncertainties of Small jets are propagated, so no more calibrations and systematic uncertainties are needed for jets with larger R. In addition, Large jets are trimmed.

Consequently the main goal of following analysis is the study of jet close-by effects and determination of their significance for jets with different radius $R = 0.2/0.4/1.0$. Based on the results it will be then considered, whether contemporarily applied jets calibrations are convenient also for multijets events under the influence of close-by effect or an additional source of systematic uncertainty should be considered. Moreover this analysis uses the jet re-clustering procedure, it is possible to decide, whether it is really safe to use the $R = 0.2$ jets for re-clusterings.

2.2 Close-by variables

The close-by effects are used to be studied using multijet p_t-balance techniques based on transverse momentum conservation. These methods are applied on the so-called back-to-back system. In concrete terms, this is about events, where the leading jet with the highest p_t is produced opposite direction to the multijets recoil system. Let us denote transverse momentum of leading jet (jet with the highest p_t in the event) as p_t^{lead} and transverse component of vector of sum of all non-leading jet momenta in recoil system as p_t^{recoil}. Hence, variable p_t-balance denoted as p_t^{Bal} could be defined as follows:

$$p_t^{Bal} = \frac{p_t^{lead}}{p_t^{recoil}} \tag{2.1}$$

In a similar way a variable response R is defined by the eq. (2.2), where the vector sum of all jet momenta in recoil system is replaced by only two members (leading jet in recoil system with momentum $\vec{p}^L$ and its nearest jet with momentum $\vec{p}^{Cl}$).

$$\text{response}\, R = \frac{(\vec{p}^L + \vec{p}^{Cl})_t}{p_t^{lead}} \tag{2.2}$$

Another variable response D is defined as in the eq. (2.3) for investigations of changes in response. However, response D does not represent a truly conserved physical variable.

$$\text{response}\, D = \frac{\vec{p}_t^L - \vec{p}_t^{Cl}}{p_t^{lead}} \tag{2.3}$$

The values of both, the response R and response D variables, should be smaller than unity by definition. In order to determine the close-by effect it is necessary to define suitable metric to describe the closeness and the isolation of jets. Classical ΔR defined by eq. (2.4) could be used for two jets.

$$\Delta R = \sqrt{\Delta^2\eta + \Delta^2\phi} \tag{2.4}$$

Where $\Delta\eta$ represents a difference in pseudorapidity and $\Delta\phi$ a difference in azimuth angle of the two considered jets. Variable ΔR will be always related to the leading jet in recoil system and its closest jet for the purpose of the interpretation in the following text.

The information about jet momenta could be also used for description of the closeness like in case of $f_{closeby}$ variable, which is defined by eq. (2.5).

$$f_{closeby}(jet) = \sum_j \frac{\vec{p}_{jet} \cdot \vec{p}_j}{|\vec{p}_{jet}|^2} \tag{2.5}$$

In general, the referenced jet in definition of $f_{closeby}$ variable is arbitrary. In case of this study, $f_{closeby}$ variable will be always computed for leading jet in recoil system (in other words for sub-leading jet in the event) and the sum will run over all remaineing jets j in recoil system with momenta $\vec{p}_j$. This variable contains scalar products of jets momenta. The individual contributions of scalar product in $f_{closeby}$ variable correspond to projection of the near jet momentum to the referenced jet momentum. Therefore, it has different behavior with respect to ΔR. Increasing $f_{closeby}$ means a decrease of ΔR and hence lesser separation. In other words jets are closer to each other with increasing $f_{closeby}$.

Slight modification of variable $f_{closeby}$ can be done for a system of only two jets. New variables f_{cl1} and f_{cl2} again related to the leading jet in the recoil system and its nearest jets are introduced by eq. (2.6) using a factor corresponding to response R.

$$f_{cl1} = \frac{\vec{p}^L \cdot \vec{p}^{Cl}}{|\vec{p}^L|^2} \cdot \text{response}\, R \qquad\qquad f_{cl2} = \frac{\vec{p}^{Cl} \cdot \vec{p}^L}{|\vec{p}^{Cl}|^2} \cdot \text{response}\, R \tag{2.6}$$

These variables f_{cl1} and f_{cl2} contain only one positive contribution, whereas $f_{closeby}$ can include positive as well as negative members of scalar products.

Since the normalization by factor $|\vec{p}^L|^2$ is always greater than $|\vec{p}^{Cl}|^2$, the range of f_{cl2} will be larger than the range of f_{cl1}. Further, the maximum value of f_{cl1} is expected to be 2. The most extreme case contains two jets in the recoil system being almost parallel to each other and exactly opposite to the referenced jet. If all three momenta will take the same magnitude, then f_{cl1} approaches 2.

Modification by response R in eq. (2.6) is introduced as otherwise when plotting response R versus $f_{closeby}$ in a particular bin of transverse momenta of leading jet p_t^{lead} the response becomes strongly dependent on $f_{closeby}$ by construction. [9] [10]

Note that the notation used in the above-mentioned definition of $f_{closeby}$ is not unified in literature focused on close-by effects. Let be emphasised here that $\vec{p}^{Cl}$ is not strictly the momentum of subleading jet, but the momentum of closest jet. The object of reference will often be specified. Further on, variable response R is often denoted as R, but it could be confusing, since the same symbol is used for the radius of jet. Therefore a full notation "response R" will be used in the following text.

2.3 Event selection

The analysis is based on the p_t balance technique, which balances the leading jet in the opposite direction to a well separated set of remaining jets. The vector sum of these jets except for the leading jet will be called as the recoil system. Events were selected using $R = 0.4$ anti-k_t jets. Events, which meet the selected criteria, were saved and further studied. The leading jets were always parameterized by radius $R = 0.4$, but recoil jets were clustered again with different radii $R = 0.2/0.4/1.0$. These recoil jets will be often denoted as Small ($R = 0.2$), Standard ($R = 0.4$) and Large ($R = 1.0$) jets. Consequently, there are three different types of recoil systems, which balances a well calibrated leading jet in the opposite direction to a well separated set of remaining jets. Detailed description of the event topology is explained at the end of this section. The objects of interests are described below.

Standard ($R = 0.4$) and Small ($R = 0.2$) jets were reconstructed from calorimeters energy clusters. There were required ${p_{tmin}}^{jet} = 25$ GeV as a minimum of transverse momentum of considered jets and detector centrality cuts $\Delta\eta_{det}$. The leading jet has to be detected in $|\Delta\eta_{det} < 1.2|$ whereas all jets in the recoil system have to be located in area $|\Delta\eta_{det} < 2.8|$. Large ($R = 1.0$) jets are a little bit different. They are built by re-clustering procedure from at least two Small ($R = 0.2$) jets. Consequently, the minimum transverse momentum of Large jets has to be 50 GeV. These Large R jets are also trimmed. The Trimming procedure (described in section 1.4.2) uses input parameters $f_{cut} = 0.05$ and $R_{sub} = 0.2$. Furthermore, jet-vertex-tagger (JVT) cut was applied on low-p_t jets, with $p_t < 50$ GeV, for pile-up subtraction. It was used $JVT < 0.64$ as a medium pile-up subtraction.

Since the following analysis studies the jet properties in wide range of transverse momenta, it was necessary to use several p_t triggers. The notation of triggers include the minimum value of p_t in GeV, from which the triggers are commonly used. Nevertheless, the p_t range of trigger were re-scaled to reach 100% efficiency. List of applied high-level triggers (HLT) is shown in Tab. 2.1 including the new re-scaled minimal transverse momenta at 100% efficiency of detection.

Further, it is important to check the data quality before the event selection. Therefore, following cleaning requirements were applied. The events, which include an incomplete or erroneous information from the calorimeters (LAr or Tile calorimeters) or Semiconductor Tracker (SCT) in the inner detector, were excluded. EventInfo::errorState and

trigger	minimal p_t at 100% efficiency [GeV]	trigger	minimal p_t at 100% efficiency [GeV]
HLT_j25	40	HLT_j175	220
HLT_j35	60	HLT_j200	260
HLT_j60	85	HLT_j260	320
HLT_j110	145	HLT_j360	440

Table 2.1: List of applied High-Level Triggers and new re-scaled minimal transverse momenta with 100% efficiency of detection.

eventInfo::isEventFlagBitSet(xAOD ::EventInfo::Core, 18) were used for *Event cleaning* and *removing incomplete events*. Since we are focused on jets created at hard collision, *Vertex-requirement* was used to reject a non-collision background events. Further suitable events have to contain at least two tracks originate from one reconstructed vertex.

The events which pass through the above-mentioned cleaning and data quality criteria were further classified by multijet event selection criteria based on MultijetBalance package. [11] The events had to include at least 3 anti-k_t $R = 0.4$ jets. The leading jet in such events also had to be located in central part of detector $|\eta_{det} < 1.2|$ with transverse momentum $p_t > 40$ GeV.

Another two more cleanings follow. *MC cleaning* is applied to remove pile-up events using Monte-Carlo slice samples. The average transverse momentum of leading jet p_t^{lead} and sub-leading jet $p_t^{sublead}$, has to be comparable with the transverse momentum of leading jet $p_{t,truth}^{lead}$ at truth particle level. It is required that $\frac{p_t^{avg}}{p_{t,truth}^{lead}} < 1.4$, where $p_t^{avg} = \frac{p_t^{lead}+p_t^{sublead}}{2}$. *Jet cleaning cut* was used, too. Jet cleaning is performed by the JetCleaningTool, which removes event, if any anti-k_t $R = 0.4$ jet does not have *clean* status.

Now, events are selected to find suitable candidates for application of multijet balance techniques. The α *cut* applies the condition on separation in azimuth angle ϕ between the anti-k_t $R = 0.4$ leading jet and the recoil system. It is demanded that $\alpha = |\Delta\phi| = |\phi_{lead} - \phi_{recoil}| > \pi - 0.3$, where ϕ_{lead} denotes azimuth angle of leading jet, whereas ϕ_{recoil} describes azimuth angle of recoil system. The α cut could be converted to $\alpha > 162.8^o$. There is one more separation condition in azimuth angle, β *cut*, which describes the isolation between the leading jet and any other jet with p_t at least one quarter of p_t^{lead}. Parameter β is defined as $\beta = \min(\Delta\phi_i) = \min(|\phi_{lead} - \phi_i|) > 1.0$, or alternatively $\beta > 57.2^o$, where the notation is the same as above and ϕ_i corresponds to azimuth angle of i-th jet with $p_t > \frac{1}{4}p_t^{lead}$. The last requirement on back-to-back system is determined by radius ΔR *cut*. It is requested that $\Delta R = \sqrt{\Delta\phi^2 + \Delta y^2} = \sqrt{(\phi_{lead} - \phi_i)^2 + (y_{lead} - y_i)^2} > 1.5$ for all anti-k_t $R = 0.4$ jets with azimuth angles ϕ_i and rapidity y_i and the leading jet at azimuth angle ϕ_{lead} a rapidity y_{lead}.

Now, finally the $R = 0.4$ recoil system could be defined as the vector sum of jets without the $R = 0.4$ leading jet. Further, these selected events will be saved and clustered again to reach new jets of radius $R = 0.2$ (Small jets). For the following analysis the leading jet will be identified with previous selection of $R = 0.4$ jet, whereas the new Small recoil system will be represented by the vector sum of new $R = 0.2$ jets, which are in a distance $\Delta R > 0.4$ from the original $R = 0.4$ leading jet. And the last, third, jet selection is done by re-clustering of $R = 0.2$ jets to new Large ($R = 1.0$) jet. The leading jet stands the same as in the previous, but the recoil system is determined by $R = 1.0$ jets except for the jets, which are within $\Delta R < 1.0$ from the original Standard ($R = 0.4$) leading jet.

The main condition refers to the detection of multijet events itself for the following analysis of close-by effects in multijet systems. Above-mentioned selection is based on Multijetbalance package [11], which contains the basic set of multijet selection criteria applied at the previous close-by jets analysis. The criteria were mostly taken and slightly extended. The framework also uses xAODAnalHelper and xAODJetReclustring packages [12] [**?**, **?**].

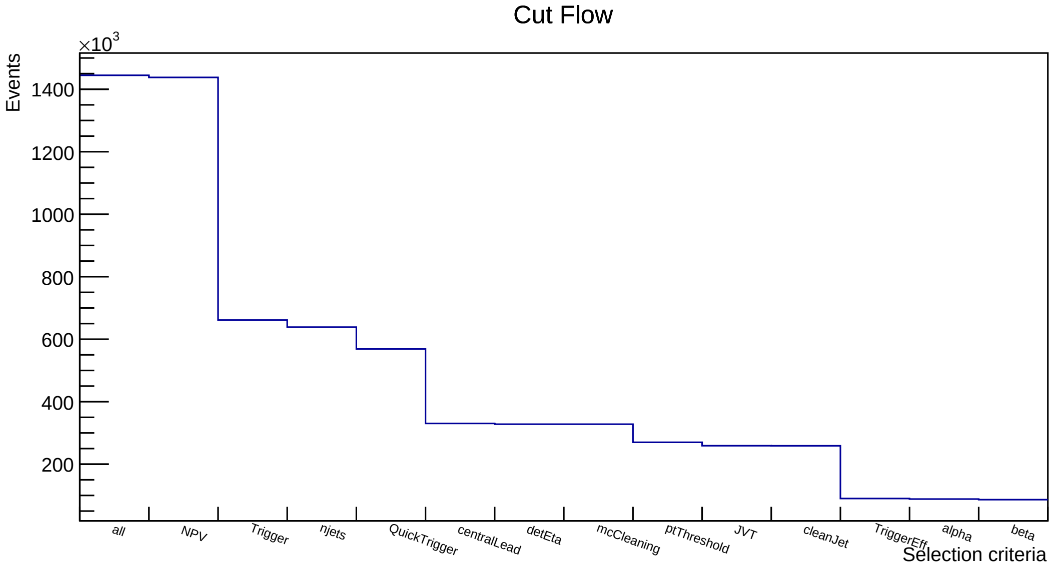

Figure 2.1: The cut-flow diagram during the events selection for one of used ATLAS data root-files. Shown selection criteria are the following in the chronological order: all- all data at the beginning of selection, NPV- events include primary vertex with at least two tracks, Triggers- High-level triggers (HLT_j25, HLT_j35, HLT_j60, HLT_j110, HLT_j175, HLT_j200, HLT_j260, HLT_j360) at the common transverse momentum range, njets- events with at leas three jets, QuickTrigger- leading jet $p_t > 40$ GeV, centralLead- centrality of leading jet ($\eta_{det} < 1.2$), mcCleaning- remove pile-up events using Monte-Carlo truth jets, ptThreshold- minimal transverse momentum of jet 25 GeV, JVT- jet-vertex-tagger for jets with $p_t < 50$ GeV ($JVT \leq 0.64$), cleanJet- JetCleanigTool, TriggerEff- 100% trigger efficiency (see Tab. 2.1) alpha- separation in azimuth angle between leading jet and recoil system, beta- separation in azimuth angle between leading jet and any jet with p_t at least $\frac{1}{4}p_t$ of leading jet.

2.4 Kinematics

The following analysis of close-by effects is built on events with well separated Standard $R = 0.4$ leading jet in the opposite direction to several non-leading jets denoted as the recoil system. These recoil systems in such type of events were studied with various radii R of jets. Therefore, the analysis uses the same sample of events, but only fraction of them were used for analysis with Small R ($R = 0.2$) and Large R ($R = 1.0$) jets, due the chosen methods for reconstruction of jets. It is also described by following distributions of jet's multiplicity in fig. 2.2.

All spectra of multiplicity in fig. 2.2 are normalized to unit area. The first distribution introduces spectrum of multiplicity of Standard ($R = 0.4$) jets, which means, that the number of jets in recoil and the leading jet are counted. Therefore multiplicity of Standard jets begins at three (at least two jets in recoil + leading jet). Whereas the spectra of Small R and Large R jets multiplicity count only jets in recoil system.

Since jets could be characterized as collimated sprays of particles, its natural that the numbers of jets decrease during the rebuilding of recoil system from original R (e.q. Standard $R = 0.4$) jets to new narrower (e.q. Small $R = 0.2$) jets. Therefore, the spectrum of multiplicity for Small R jets in recoil does not start at value 2. The recoil system have to count at least two $R = 0.4$ jets, nevertheless number of Small R ($R = 0.2$) jets is not specified. Therefore Small R jet's multiplicity could start at zero. Even so, there is approximately 25% probability that the recoil of Small R jets should not be built. In the other words, narrower jets do not contain enough transverse momenta frequently (energy respectively) to pass the minimal transverse momentum criterion $p_{t_{min}}^{jet}$. It also corresponds to the multiplicity spectrum of Large R jets. If not at least two of Small R jets are present then the re-clustering procedure cannot be used for construction of the Large R jet. In such case the Large R jet could create a recoil system itself. The jet's multiplicity shows significant decreasing of jets at the beginning of distribution. For instance the variable f_{cl2}, which quantifies mutual closeness of Sub-leading jet in recoil system and the closest jet on recoil, will be computed from less than 30 % of all selected events with Standard R ($R = 0.4$) recoil jets in case of Small R recoil jets. Similarly only 5 % of original events were used to compute f_{cl2} variable in case of Large R recoil jets. That can indicate possible problems with statistics for results of Large R jets at low-pt analysis.

Denote, high jets multiplicity is not well described by Pythia. The ratio of data and Pythia prediction decreases lower then 0.5 for six jets and more. Thus Pythia Monte-Carlo generator is not suitable for description of process covering high number of jets as for example heavy boosted Z' boson decay. That is caused by Pythia's computation of matrix elements in the leading order, which does not consider higher orders of perturbative calculus. For such instances are more suitable Herwig^{++} or Powheg Monte-Carlo event generators.

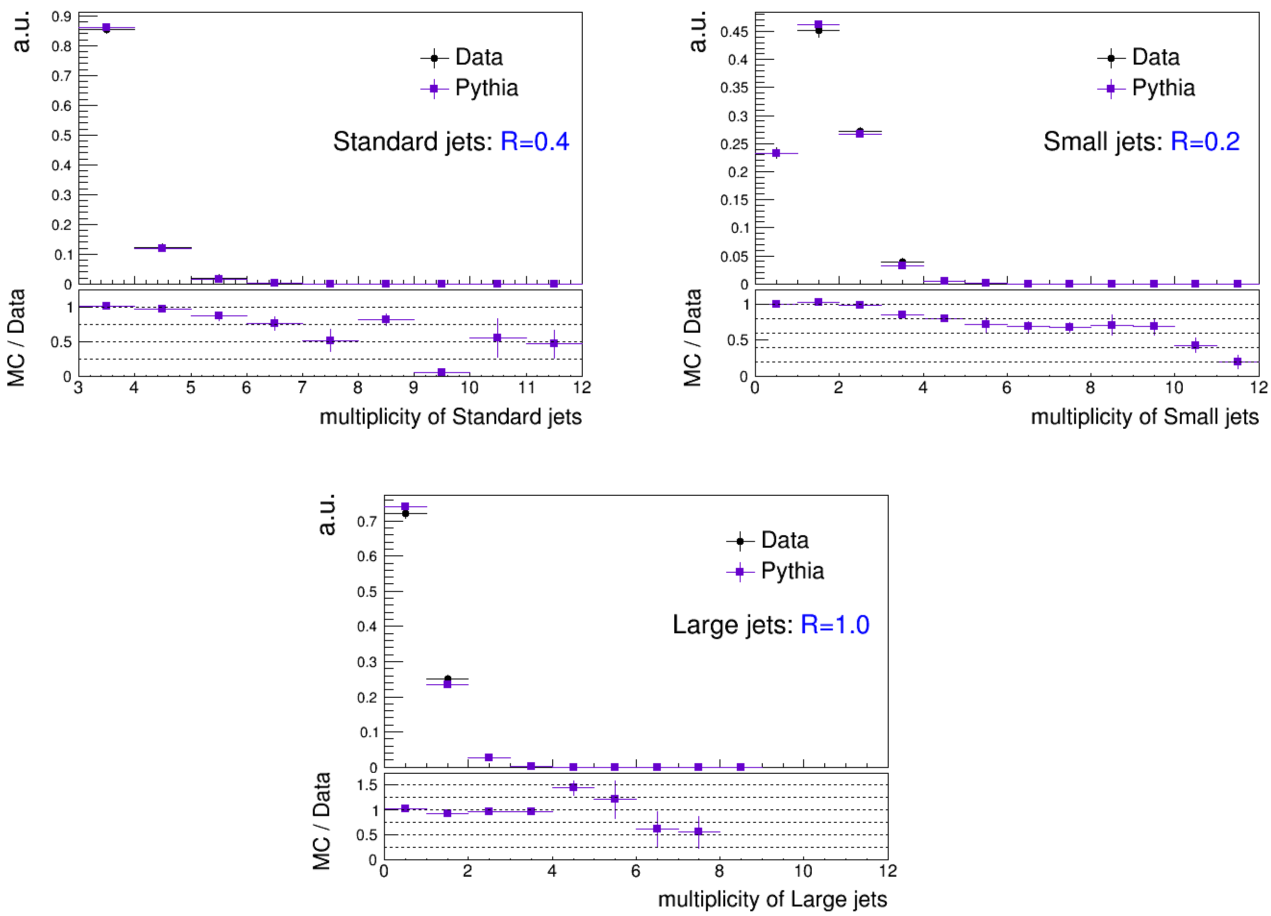

Figure 2.2: Spectra of jet's multiplicity normalized on unit area for Standard ($R = 0.4$), Small ($R = 0.2$) and Large ($R = 1.0$) jets. Multiplicity of Standard R jets (left) counts number of jets in recoil system and itself leading jet, whereas distribution of Small R (middle) and Large R jets (right) contain only jets in the recoil system. ATLAS data are compared with Pythia Monte-Carlo generator. Only statistical uncertainties are shown.

2.5 Close-by effects at high-p_t scale

This section represents the results of the analysis, which was focused on close-by effects of jets in multijet events. Most of shown dependencies were constructed from multidimensional histograms, which were splitted to required intervals of observed variables. Mostly was studied the development of balance variables and their dependency on distance of two closest jets and the transverse momentum of leading jet in event. Therefore, mostly $3D$ histograms were used. First cycle of slices leads through momenta of leading jet, the second one runs over the close-by variable of distance, which describes relative distances of two objects. That way was obtained a spectrum of some types of balance variables in specified range of distance metric and transverse momenta of leading jet. Such spectrum was frequently described by symmetric Gaussian distribution. If the spectrum could be fitted by Gaussian, then the mean value of Gaussian fit was plotted to final graph at associated range of close-by distance variable. If the spectrum did not correspond to Gauss distribution, but still disposed with high statistic, the mean of histogram was extracted. This method was used bin-by-bin to obtaine final graph of wanted distributions: some type of balance variable vs. close-by metric vs. p_t of the leading jet.

The vast majority of dependencies we were interested in represented the response R variable (defined by eq. 2.2) as a function of ΔR (distance between the leading jet in recoil and its the closest jet in (ϕ, y) coordinates) or f_{cl1} close-by metric (close-by variable as a distance variable between the leading jet in recoil and its the closest jet) or f_{cl2} respectively (close-by variable between sub-leading jet in recoil and its closests jet). The different uses of metrics for quantification of close-by effect are defined by eq. 2.4 and eq. 2.6.

The first set of final distributions are shown below. It represents the dependecy of response R vs. different close-by metrics vs. of leading jets for all three types of jets ($R = 0.2/0.4/1.0$) in recoil systems. The results are represented firstly for high-p_t analysis of the leading jet (from 200 GeV to 1000 GeV in 200 GeV intervals). The second set of results corresponds to low-p_t intervals of leading jet (from 40 GeV to 200 GeV in 40 GeV intervals), which will be shown and discussed in next section.

The first results of close-by effects show fig. 2.3, 2.4, 2.5 at high-p_t scale ($200 - 1000$ GeV) of leading jet, where response R vs. ΔR vs. $p_t(lead)$ of leading jet dependency are represented. These three sets of graphs are associated with three different sets of jets in recoils system in radius order: Small ($R = 0.2$), Standard ($R = 0.4$) and Large ($R = 1.0$) recoil jets. Each set includes four distributions, which are differentiated by transverse momenta of leading jet $p_t(lead)$. Some of the collections were not supported by sufficient amount of data, thus they cover only 3 or 2 distributions. Analogical scheme of results representation is also used for the rest of the close-by metrics (ΔR, f_{cl1}, f_{cl2}).

At the first denote, the close-by effects are identified as a change of shape in graphs of some kinds of balance variable as a function of distance. Therefore the exact value of balance variable is not fundamental, we need to focus on the trend and its evolution instead. Nevertheless it is important to keep studying in (correctly) balanced system. Therefore, all of response R distributions at high-p_t analysis show reasonable results, since all response R distributions are less than 1.0 for all close-by distance variables (ΔR, f_{cl1} and f_{cl2}). That corresponds with the definition eq. (2.2) itself. In other words, the transverse momentum of sub-leading jet (leading jet in recoil) and it's closest jet contain only a fraction of the whole recoil system, which is equal or less than p_t of leading jet.

The collections of fig. 2.4 2.5 which contain Standard R and Large R recoil jets show almost constant dependence for all transverse momenta $p_t(lead)$ intervals from 200 GeV to 1000 GeV, therefore we do not observe any close-by effects. In case of ΔR distribution, only fig. 2.3 contains inconstant trend, which could be interpreted as out-of cone energy deposition, which could still increase the overall p_t of recoil jets. With increasing mutual distance of the closest jets, jets become more separated. Therefore these jets absorb less particles as well as radiation. The raising trend of response R in case of Small jets in fig. 2.3 is located at $\Delta R \approx 0.4$, in other words at the double value of the radius parameter of Small ($R = 0.2$) jets in recoil system. This indicates that close-by effects are indeed observed, especially for jets that touch each other.

The next distributions of response R are seen in fig. 2.6, 2.7,2.18. There are shown the dependencies of response R vs. f_{cl1} vs. p_t of leading jet for all three radii of jets in recoil system. Unlike the previous ΔR distributions, where jets are less separated with decreasing ΔR, here are jets less separated with increasing f_{cl1}. The advantage of f_{cl1} variable is including the information about jets momenta. Since the f_{cl1} is not linear function of ΔR, it is more sensitive to close-by effects. The shown spectra display very slightly increasing trend dependency (almost constant) on Standard and Large R jets in recoil. In case of Small R jets, the dependences increase faster than in case of Standard and Large R jet distributions. Also, it is possible to observe a general trend of decreasing transverse momentum of leading jets, when the close-by effects become more visible. It is nature, due to the results of the jet shapes, which quantifies the amount of transverse momenta inside the jets as a function of distance ΔR measured from the jet's axis. Results of these studies imply, that jets become more collimated with increasing p_t of jet.

Results of the last studied distance metric f_{cl2} are shown in fig.2.9, 2.10, 2.11. Since f_{cl2} variable has similar constructions as the f_{cl1} the distributions of response R vs. f_{cl2} vs. $p_t(lead)$ of leading jet performs analogical results. Close-by effects are visible in case of Small R jets in fig. 2.9 and most visible in graphs with the lowest $p_t(lead)$ (in range $200-400$ GeV). Other graphs (associated with Standard and Large radius recoil jets in fig. 2.10 2.8) do not include observable close-by effects.

We wish to stress that all results in this chapter are found in a perfect agreement with those presented in ATLAS note [10].

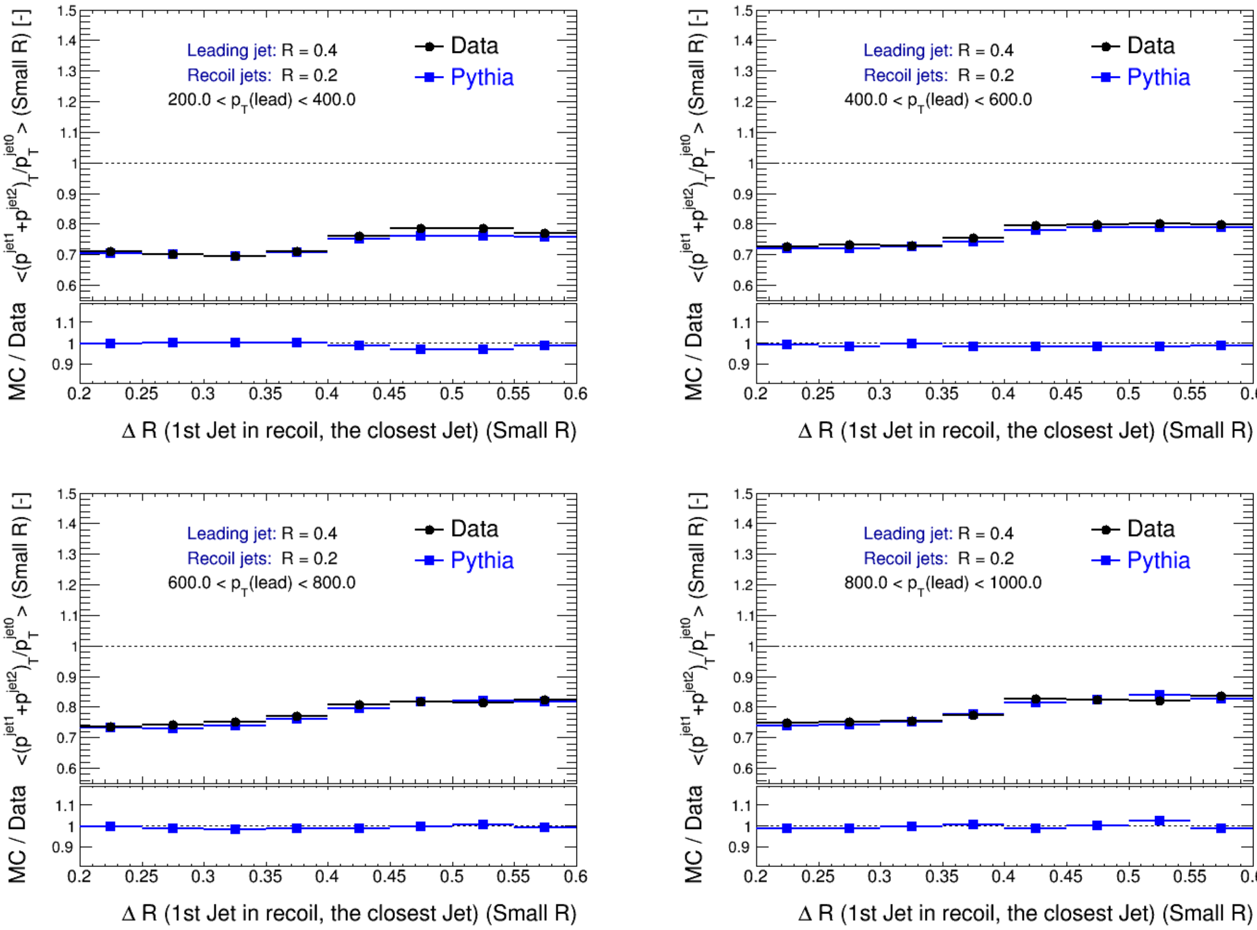

Figure 2.3: Comparison of response R spectra from Gaussian fit as a function of the ΔR and transverse momentum of leading jet $p_t(lead)$ for ATLAS data and MC Pythia 8. All spectra are associated with recoil system formed of $R = 0.2$ (Small) jets. Response R is shown in four bins of $p_t(lead)$: $(200 - 400)$ GeV (top-left), $(400 - 600)$ GeV (top-right), $(600 - 800)$ GeV (bottom-left) and $(800 - 1000)$ GeV (bottom-right).

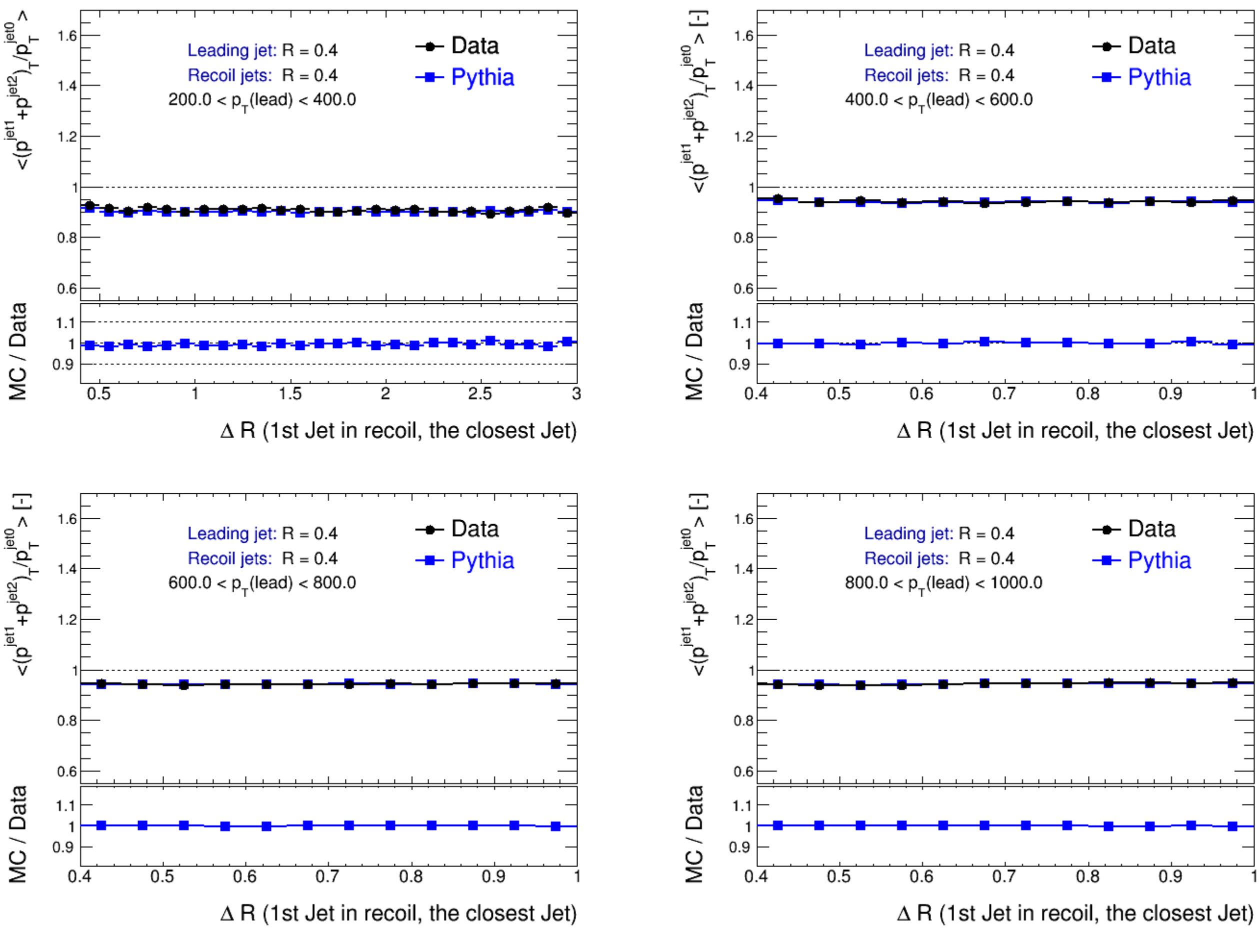

Figure 2.4: Comparison of response R spectra from Gaussian fit as a function of the ΔR and transverse momentum of leading jet $p_t(lead)$ for ATLAS data and MC Pythia 8. All spectra are associated with recoil system formed of $R = 0.4$ (Standard) jets. Response R is shown in four bins of $p_t(lead)$: $(200-400)$ GeV (top-left), $(400-600)$ GeV (top-right), $(600-800)$ GeV (bottom-left) and $(800-1000)$ GeV (bottom-right)..

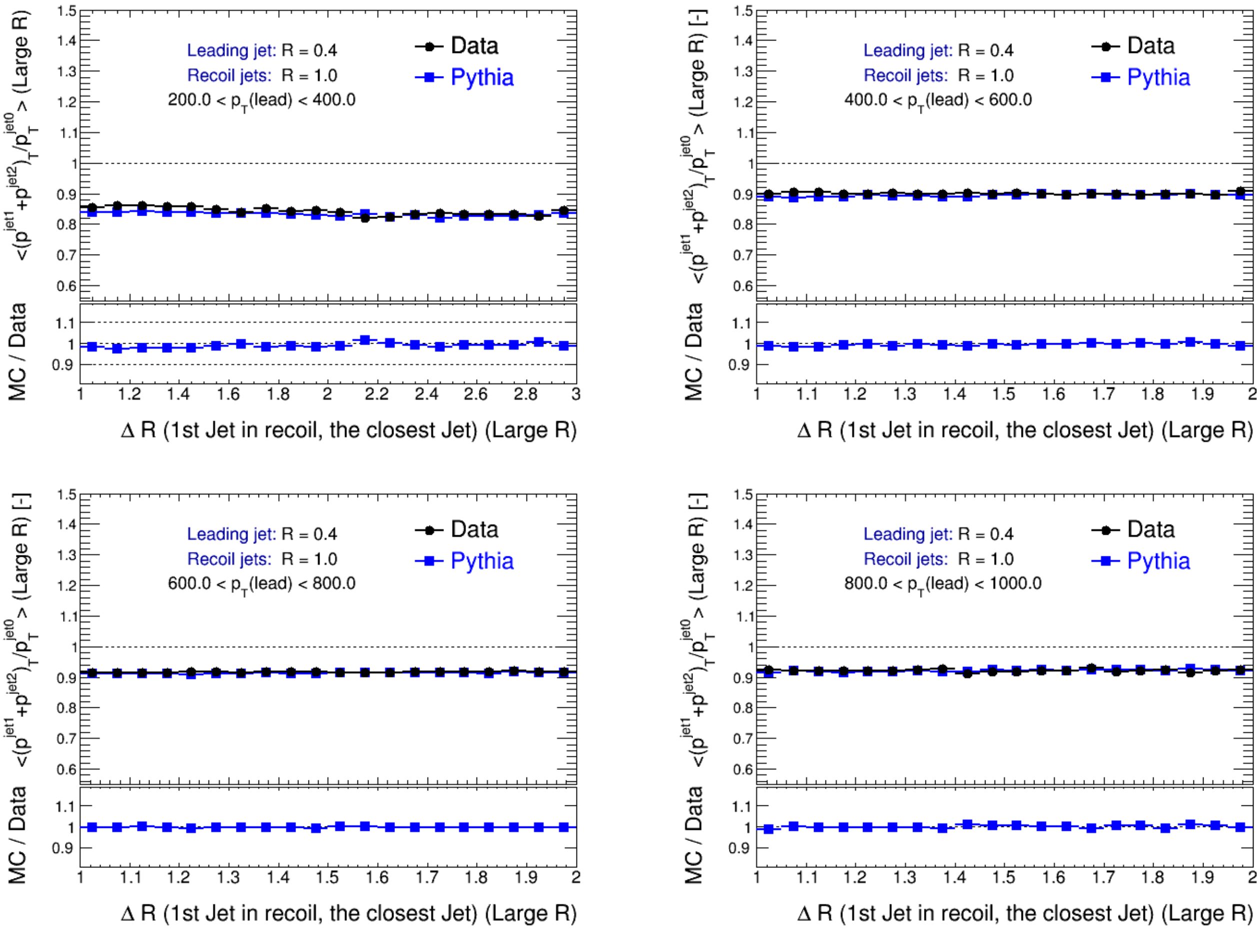

Figure 2.5: Comparison of response R spectra from Gaussian fit as a function of the ΔR and transverse momentum of leading jet $p_t(lead)$ for ATLAS data and MC Pythia 8. All spectra are associated with recoil system formed of $R = 1.0$ (Large) jets. Response R is shown in four bins of $p_t(lead)$: $(200 - 400)$ GeV (top-left), $(400 - 600)$ GeV (top-right), $(600 - 800)$ GeV (bottom-left) and $(800 - 1000)$ GeV (bottom-right).

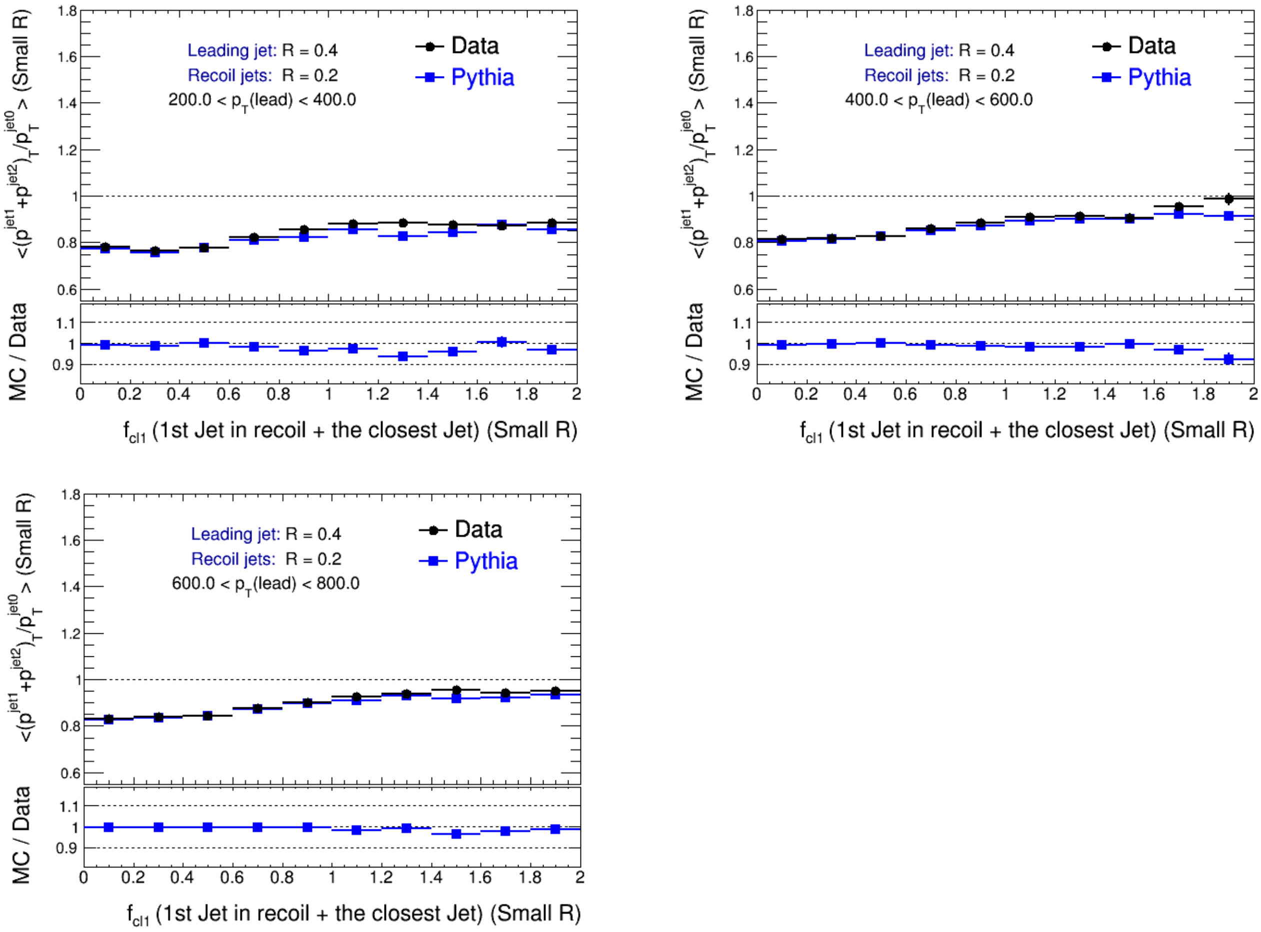

Figure 2.6: Comparison of response R spectra from Gaussian fit as a function of the f_{cl1} and transverse momentum of leading jet $p_t(lead)$ for ATLAS data and MC Pythia 8. All spectra are associated with recoil system formed of $R = 0.2$ (Small) jets. Response R is shown in four bins of $p_t(lead)$: $(200 - 400)$ GeV (top-left), $(400 - 600)$ GeV (top-right) and $(600 - 800)$ GeV (bottom-left).

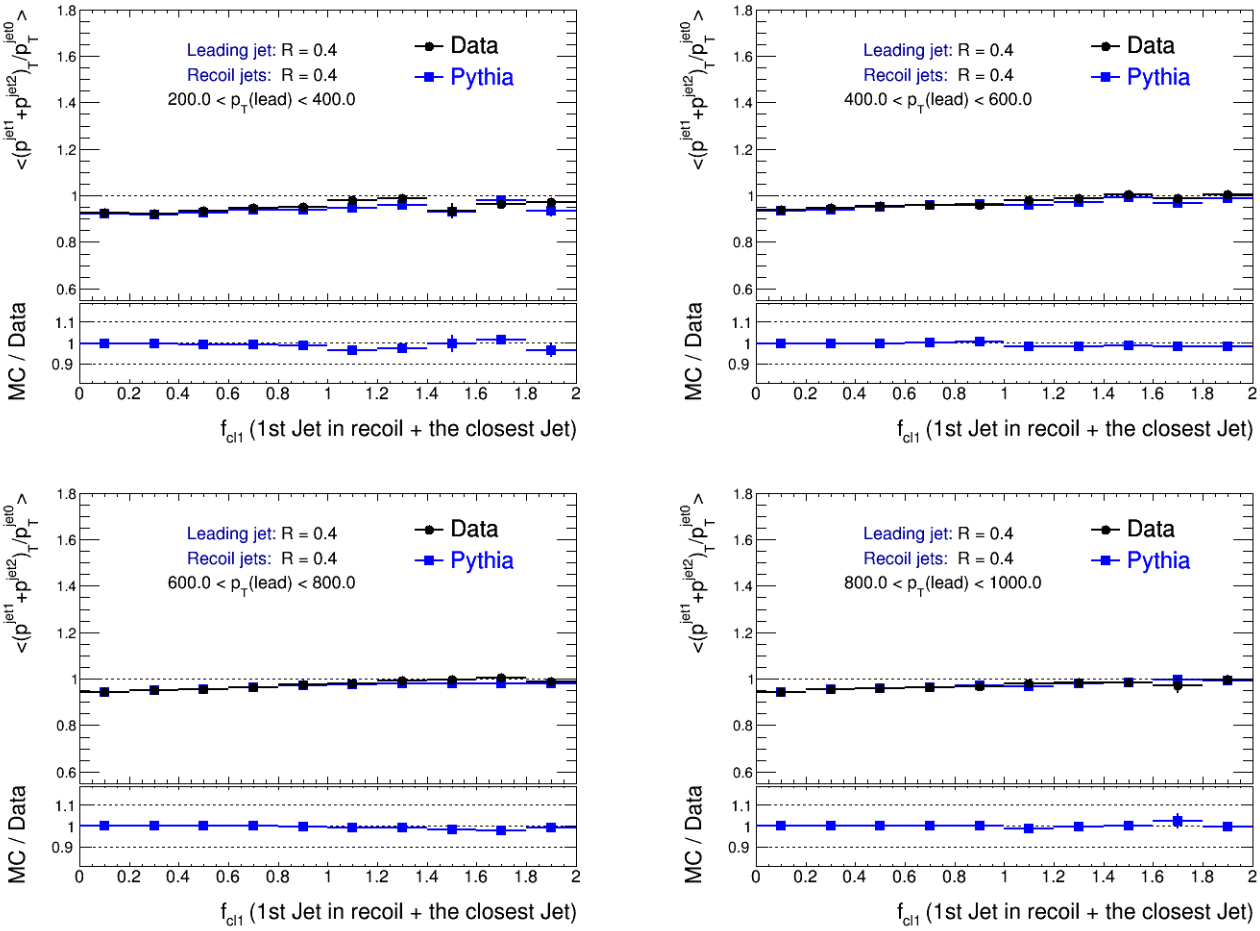

Figure 2.7: Comparison of response R spectra from Gaussian fit as a function of the f_{cl1} and transverse momentum of leading jet $p_t(lead)$ for ATLAS data and MC Pythia 8. All spectra are associated with recoil system formed of $R = 0.4$ (Standard) jets. Response R is shown in four bins of $p_t(lead)$: $(200-400)$ GeV (top-left), $(400-600)$ GeV (top-right), $(600-800)$ GeV (bottom-left) and $(800-1000)$ GeV (bottom-right).

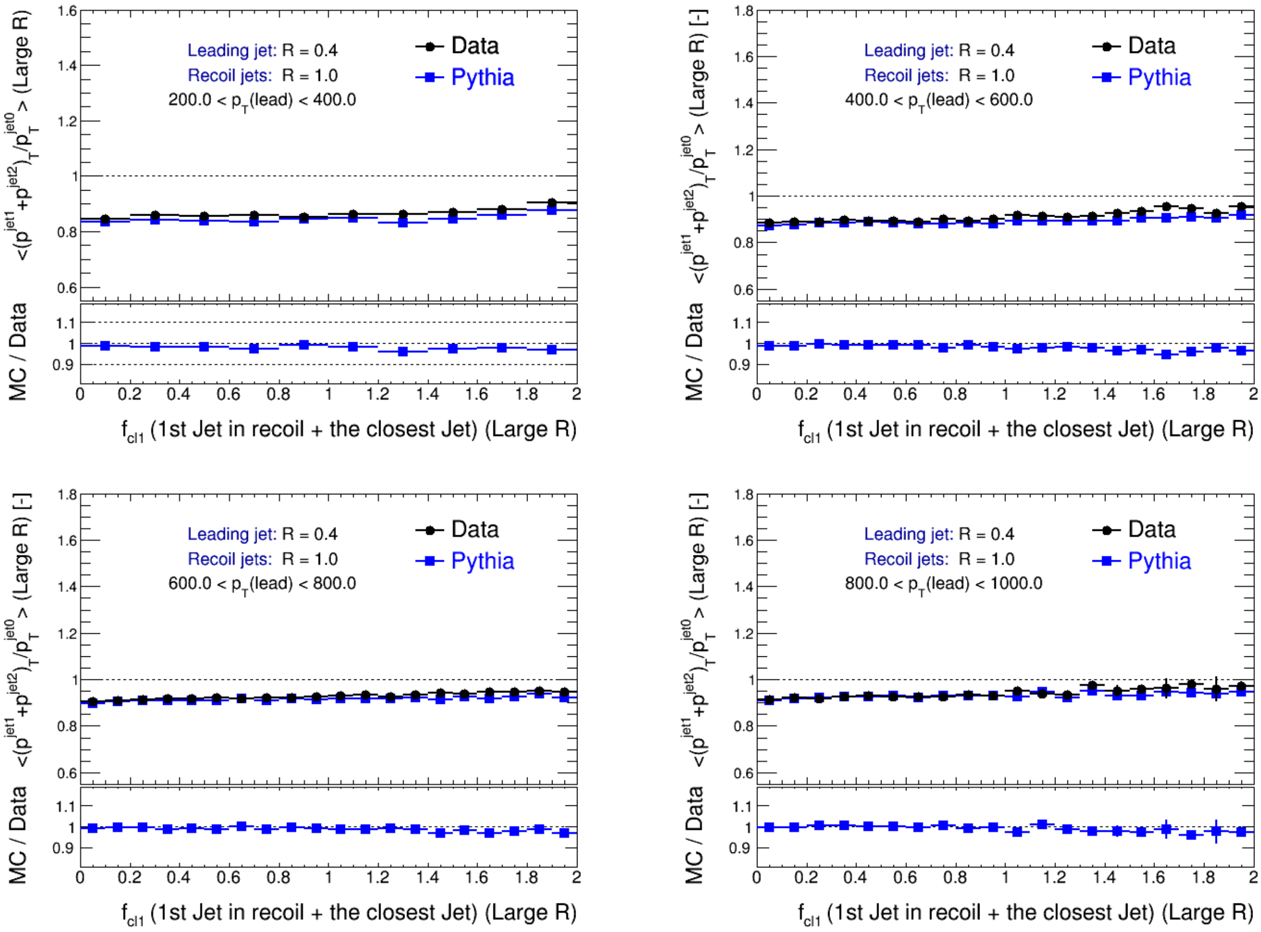

Figure 2.8: Comparison of response R spectra from Gaussian fit as a function of the f_{cl1} and transverse momentum of leading jet $p_t(lead)$ for ATLAS data and MC Pythia 8. All spectra are associated with recoil system formed of $R = 1.0$ (Large) jets. Response R is shown in four bins of $p_t(lead)$: $(200-400)$ GeV (top-left), $(400-600)$ GeV (top-right), $(600-800)$ GeV (bottom-left) and $(800-1000)$ GeV (bottom-right).

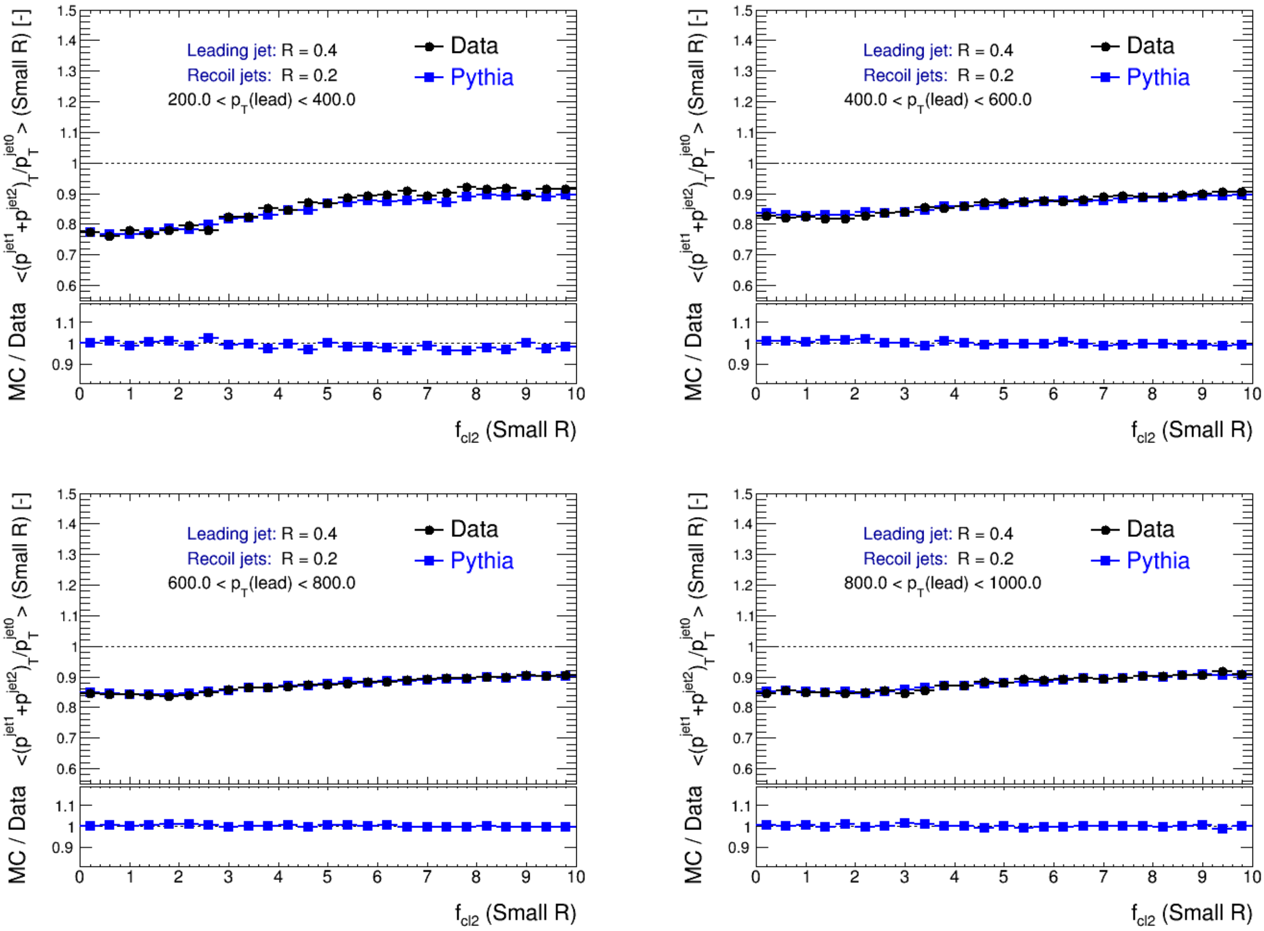

Figure 2.9: Comparison of response R spectra from Gaussian fit as a function of the f_{cl2} and transverse momentum of leading jet $p_t(lead)$ for ATLAS data and MC Pythia 8. All spectra are associated with recoil system formed of $R = 0.2$ (Small) jets. Response R is shown in four bins of $p_t(lead)$: $(200 - 400)$ GeV (top-left), $(400 - 600)$ GeV (top-right), $(600 - 800)$ GeV (bottom-left) and $(800 - 1000)$ GeV (bottom-right).

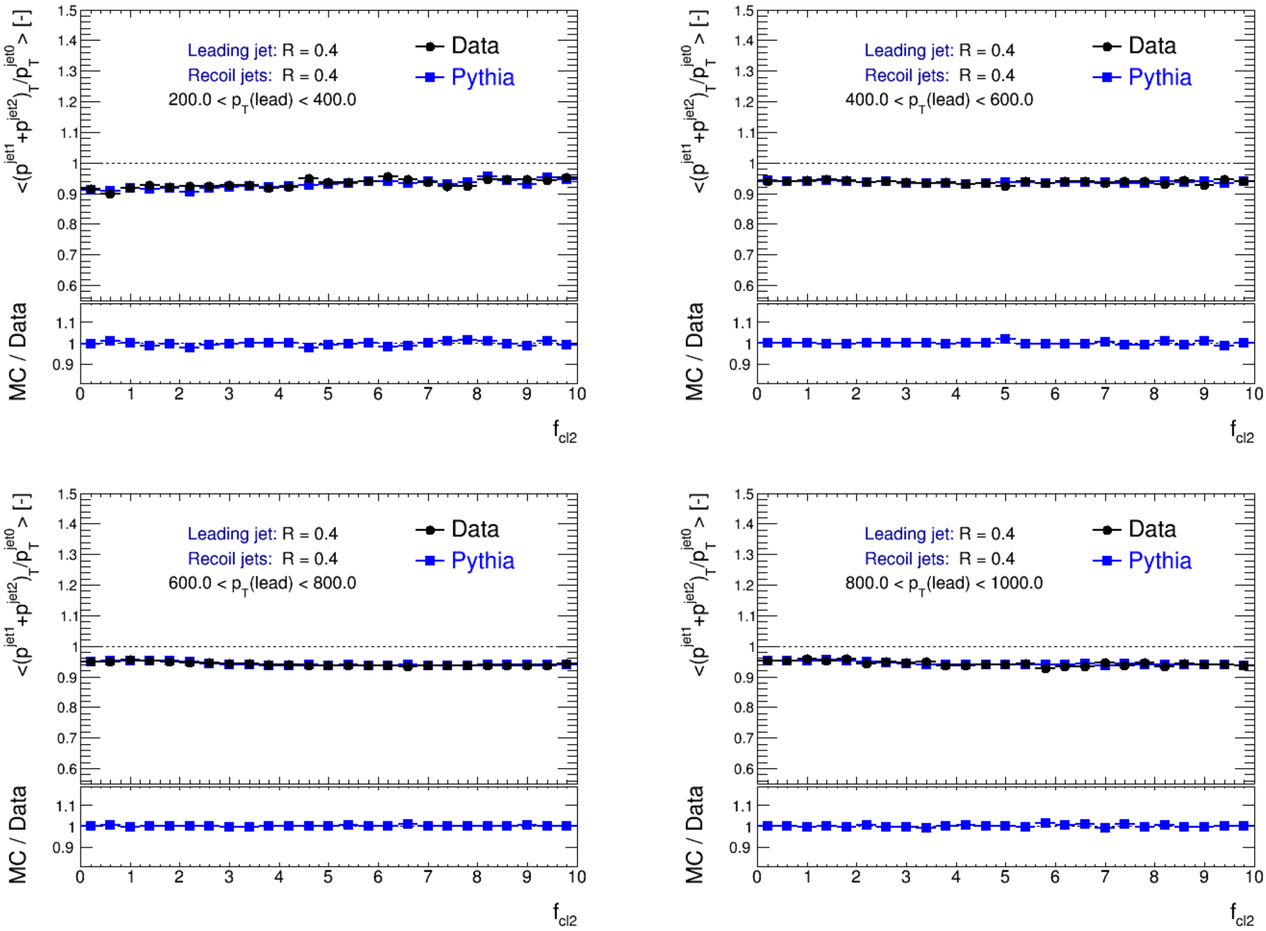

Figure 2.10: Comparison of response R spectra from Gaussian fit as a function of the f_{cl2} and transverse momentum of leading jet $p_t(lead)$ for ATLAS data and MC Pythia 8. All spectra are associated with recoil system formed of $R = 0.4$ (Standard) jets. Response R is shown in four bins of $p_t(lead)$: $(200-400)$ GeV (top-left), $(400-600)$ GeV (top-right), $(600-800)$ GeV (bottom-left) and $(800-1000)$ GeV (bottom-right).

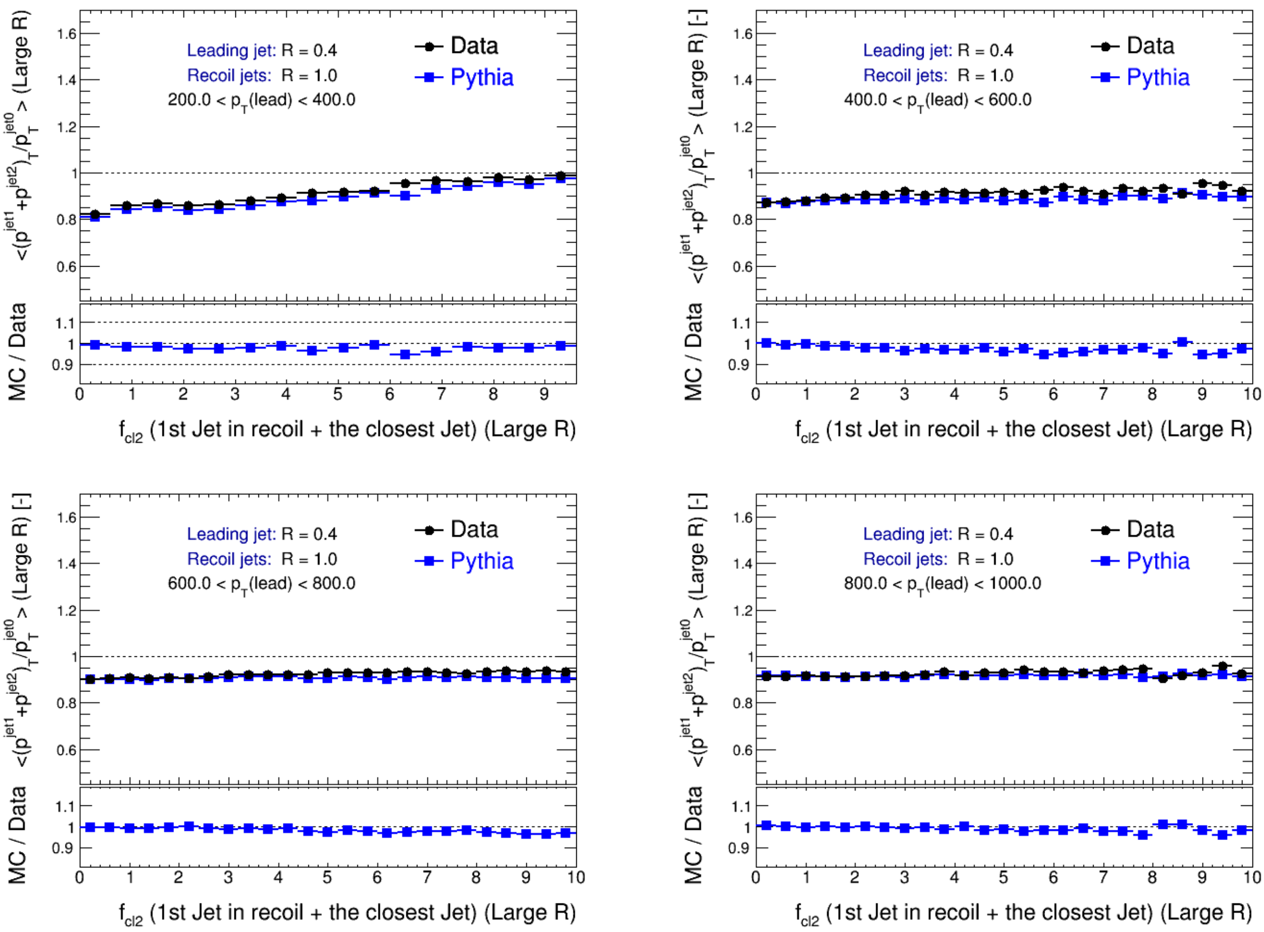

Figure 2.11: Comparison of response R spectra from Gaussian fit as a function of the f_{cl2} and transverse momentum of leading jet $p_t(lead)$ for ATLAS data and MC Pythia 8. All spectra are associated with recoil system formed of $R = 1.0$ (Large) jets. Response R is shown in four bins of $p_t(lead)$: $(200 - 400)$ GeV (top-left), $(400 - 600)$ GeV (top-right), $(600 - 800)$ GeV (bottom-left) and $(800 - 1000)$ GeV (bottom-right).

2.6 Close-by effects at low-p_t scale

The same study of close-by effects was done again, but now focused on the region of $p_t(lead)$ below 200 GeV. The lowest p_t reached value of 40 GeV, because 40 GeV represents a threshold of the lowest p_t of High Level Trigger (HLT) above which a 100% trigger efficiency is achieved. In fact, the lowest considered transverse momentum of jet corresponds to 25.0 GeV, nevertheless further cut on 100% detection probability of the leading $R = 0.4$ jet starts at 40.0 GeV. Therefore, this section will be focused on relation of response R vs. different distance variables vs. $p_t(lead)$ in range $40 - 200$ GeV. Results are presented in intervals of 40 GeV of $p_t(lead)$. More details about 100 % HLT trigger efficiency are stated in Tab. 2.1.

Note that, this part of the thesis represents the extension of close-by effects analysis of jets, which was performed by R. Lysák and J. Hejbal [10]. Their work served as a basis for the analysis in this thesis. In the previous section we verified that results for jets of high p_t are in a full agreement with those presented in ATLAS Note [10]. Further, the previous section was done as reproduction of their results and verifies the correct function of the framework for the following low-p_t analysis.

In case of low-p_t analysis, statistics fluctuations were observed in $2D$ spectra for fitting. Therefore, individual access was necessary for single fitted spectra. Expansion of bins and *individual fit procedure* were used, which is described below. If the spectrum did not contain enough data (typically less than three bins with reasonable statistics), then the spectrum could not be used to extract mean values. Hence, these intervals of close-by variables were ignored and not included in the final graphs. Otherwise, ideal range of Gaussian fit was seeked to compute the mean of Gaussian and corresponding uncertainty. Parameter of goodness of fit, χ^2 per degree of freedom, were used to find the best choice of fit range. The final choice of fitted interval as well as the fit itself was found during a manual cycle over considered ranges of fit. If Gaussian did not fit data with sufficient exactness, Chi^2 per degree of freedom reached too distant values from unity at any range of fitted interval, then the mean of histogram was plotted to the final graph. Denote, the mean of the histogram was used only in few cases, mostly in the last bins of response R vs. close-by metric vs. $p_t lead$ in problematic intervals of $p_t(lead)$: $40 - 80$ GeV and $80 - 120$ GeV. This *individual fit procedure* was used bin-by-bin to determine individual mean values of balance variable (response R) at specific range of close-by distance variable (ΔR, f_{cl1} ,f_{cl2}) and at specific range $p_t(lead)$ in low-p_t scale analysis.

As it was written above, merging of some bins had to be used, which might have decreased the resolution. Therefore, bins do not have the same range in each distance variable in the following response R spectra as in the previous section. Because the procedure of the decrease of the number of bins starts at the beginning of the spectrum, the last set of data might not be shown. In case of ΔR, the highest values correspond to the well separated jets, so no information about close-by effects is lost. Further, in case of f_{cl1} and f_{cl2} spectra, the closest jets are observed in high values of close-by distance. Notwithstanding, data for the closest jets at problematic low-p_t bins (usually in $40 - 80$ GeV) are often absent. Therefore, no information of close-by effects is lost because of merging of bins.

The distributions of response R vs. distance ΔR (distance in (ϕ, y) coordinates between the leading jet in recoil and its the closest jet) in different bins of $p_t(lead)$ is presented by fig. 2.13 2.14 2.15. Similarly as in the previous section, each set of graphs is associated with one radius R of jets in recoil system. The sets of graphs are presented in the following order: Small ($R = 0.2$), Standard ($R = 0.4$) and Large ($R = 1.0$) recoil jets.

The first set corresponding with ΔR distributions shows the unexpected dependency. The response R exceeds the value of 1.0 in the area of lowest $p_t(lead)$ of $40 - 80$ GeV for Small R and Standard R recoil jets, which is in conflict with the definition eq.2.2. Yet, we are able to explain this bizarre dependency due to selective criteria mentioned above. In fact, events with the lowest $p_t(lead)$ cannot be well balanced if, for instance, a selected event disposes of a leading jet of $p_t(lead) \approx 40$ GeV, which is situated at the opposite of the recoil system, which includes two jets of $p_t \approx 25$ GeV. In such a case, the sum of p_t sub-leading jet $p_t(subLead)$ and of 3rd jet $p_t(3rd)$ makes it ≈ 50 GeV. Therefore, the relative transverse momentum

$\frac{p_t(lead)}{p_t(subLead)+p_t(3rd)}$ (with regard to the leading 40 GeV jet) corresponds to a 1.25. It might be true that the response$R$ is not defined as a mere sum of p_t but as a transverse projection from vector sum of subleading jet's momentums and its closest jet. Yet, it is possible to make such an estimate with approx. 10% of uncertainty. After all, the insufficient balance of low-p_t might be visible in the graph for p_t-Balance (defined by eq 2.1) with dependencies on a transverse momentum of a leading jet on the fig. 2.12. The p_t-balance draws near 1.0 in the case of a well-balanced system. The presented p_t-Balance spektra show the following general trend. The recoil system becomes less balanced with decreasing p_t of leading jet. Events balanced in the best way are the ones with Standard R jets. In their case, the deviation (transverse momentum of the vector sum of all jets in a recoil system from p_t of leading jet) is only $2-4$ % in the whole observed area. The p_t-Balance grows significantly with decreasing $p_t(lead)$ in spectra of Small R and Large R recoil jets. The overall p_t of the recoil system pt^{recoil} is by 25% larger than $p_t(lead)$ in selected events with $p_t(lead) = 50-100$ GeV. Due to the fact Large jets are built by the re-clustering of Small R jets, the spectrum of Large R jets describe very similar dependency. Primarily, the analysis was prepared for the study of jet with $p_t < 1000$ GeV, therefore, we observe an even dependency in this kinematic range. While in the area above 1000 GeV, all the necessary correction are not included and that is why the fluctuation might be observed.

The next results of close-by effects are shown in plots of response R vs. f_{cl1} vs. $p_t(lead)$ in fig. 2.16 2.17 2.18. Results are consistent with an observation stated above in ΔR spectra. Similar dependencies are seen in graphs of response R vs. f_{lc2} vs. $p_t(lead)$ in fig. 2.19 2.20 2.21 for all three sets of recoil jets with radii R=0.2/0.4/1.0.

The following dependencies can be observed by mutual comparison of fig. 2.13 2.14 2.15 2.16 2.17 2.18 2.19 2.20 2.21. However, it could be more visible by using graphs in fig. 4.1, 4.2, 4.3, which are located in back-up. These figures contain the same dependencies as the previous response R distributions, but these ones are more compact. Since they show dependencies of all three types of recoil jets in one plot at considered metric and $p_t(lead)$, the slight differences will be more visible.

Concerning the set of all low-p_t plots of response R for the three radii of the recoil jet, we make the following observations: the response R approaches unity with increasing jet radius (for a fixed interval of $p_t(lead)$) for all studied variables ΔR, f_{cl1} and f_{cl2}. Very similar shapes of response R are observed in the middle of the interval of ΔR for all jet radii, the shapes only are vertically shifted by a constant. The response R for Standard and Large jets are higher than those for the Small jets which means the former are better balanced. The $p_t(lead)$ interval $40-120$ GeV where response R exceeds unity was discussed earlier. The shapes start to differ at the beginnings and ends of the spectra where jets are supposed to be closest (resp. farthest) to each other. The response R for various jet collections converge to each other for $p_t(lead) > 160$ GeV not only at the middle but also at the smallest mutual jet distances (small ΔR and large f_{cl1} and f_{cl2}). We also conclude that values of response R increase with decreasing $p_t(lead)$ and response R finally exceeds unity for the lowest $p_t(lead)$.

Now, the observed dependencies will be discussed with the respect of the transverse momenta of leading jet $p_t(lead)$. The results verify the prediction that the close-by effects become more significant (visible) with increasing $p_t(lead)$. It is evident almost from every set of response R graphs in high-p_t scale analysis and distributions of $p_t(lead)$ in $120-160$ GeV and $160-200$ GeV. However, the close-by effects of Small R and Standard R jets appear comparable in first two intervals of $p_t(lead)$ for all studied metrics. Consequently, the visible increase of close-by effects is not observed here as it was expected in lowest $p_t(lead)$ bins $40-80$ GeV and $80-120$ GeV. Unfortunately, Large R jets were not reconstructed at so low $p_t(lead)$ intervals. Leastwise rough idea can be provided by distributions of ΔR and f_{cl1} distributions for in $p_t(lead)$ $80-120$ GeV.

Further, it seems, the close-by effects are the most significant for Small ($R = 0.2$) jets from comparison of f_{cl1} and f_{cl2} distributions at $120-160$ GeV and $160-200$ GeV intervals of $p_t(lead)$. The close-by effects of Standard and Large R jets become almost the same and less important than for Small R jets in these two $p_t(lead)$ intervals. Even the response R distributions are mostly overlapped for Standard and Large R jets in graphs with $120-160$ GeV and $160-200$ GeV of $p_t(lead)$.

Compared to Monte-Carlo samples Pythia 8 the data differs by less than 5%. Higher deviations are observed only in the last bins of ΔR distributions associated with very well separated jets, which are not so important for the study. Further, higher differences could be observed in the last bins of f_{cl1} and f_{cl2} distributions, where a significant statistic uncertainties are also observed.

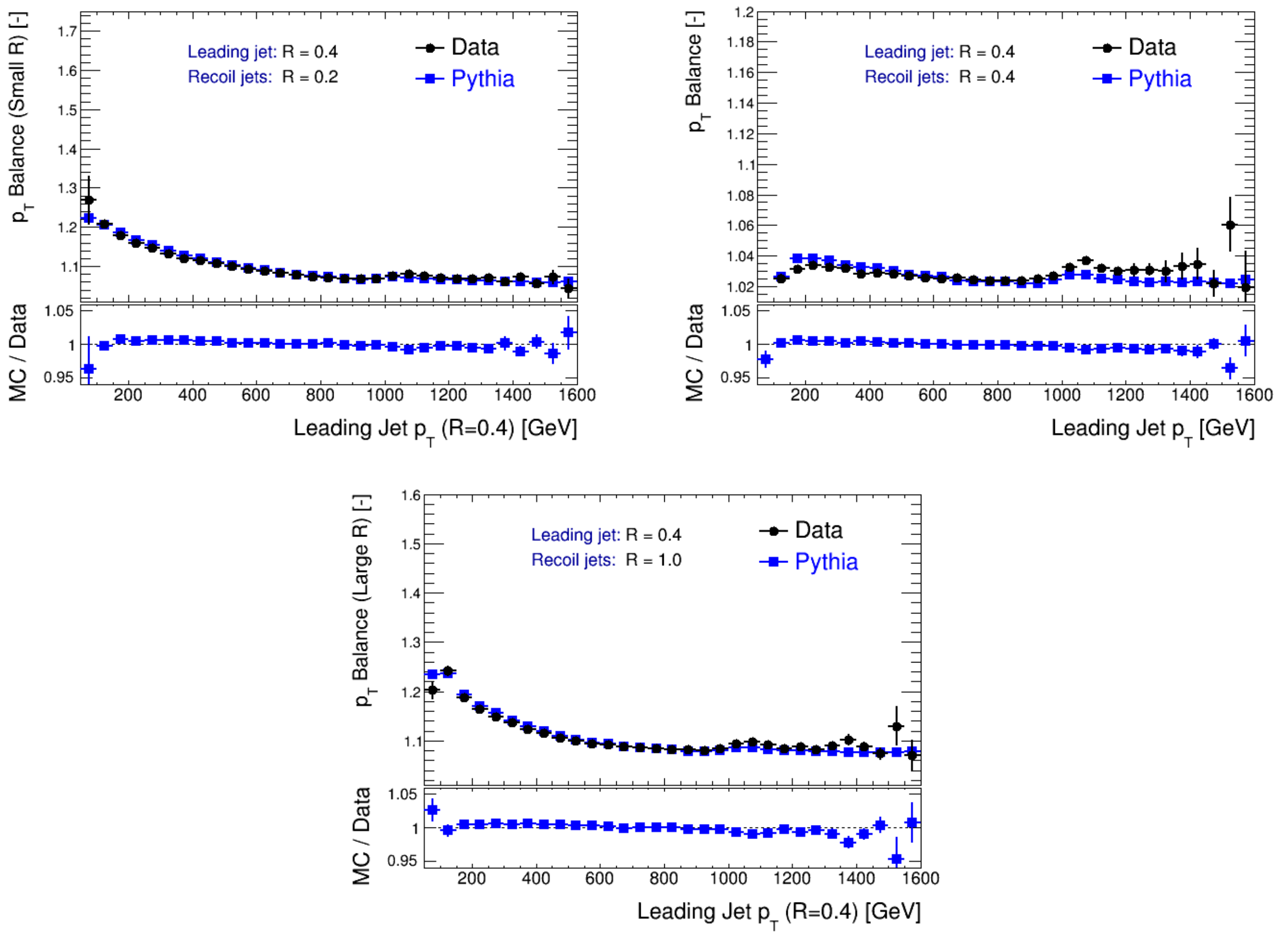

Figure 2.12: The p_t-Balance spectra as a function of transverse momentum of leading jet $p_t(lead)$ for Standard ($R = 0.4$) leading jets. Distributions show comparison for tree types of jets in recol system: Small ($R = 0.2$) recoil jets (top-left), Standard ($R = 0.4$) recoil jets (top-right), Large ($R = 1.0$) recoil jets (bottom-middle). Comparison is made for ATLAS data and prediction of MC generator Pythia 8.

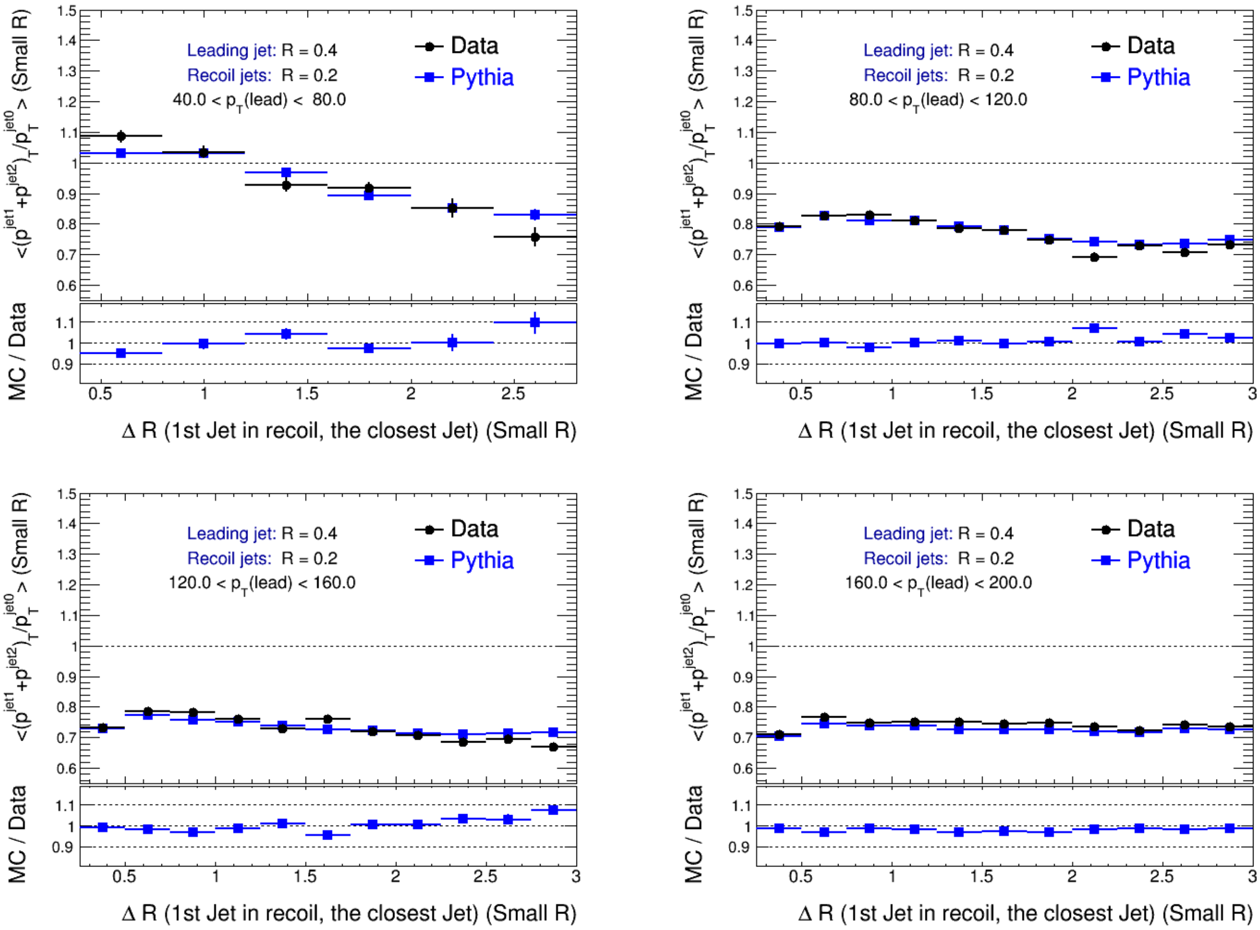

Figure 2.13: Comparison of response R spectra as a function of the ΔR and transverse momentum of leading jet $p_t(lead)$ for ATLAS data and MC Pythia 8. Response R values were reached by *individual fit procedure*. All spectra are associated with recoil system formed of $R = 0.2$ (Small) jets. Response R is shown in four bins of $p_t(lead)$: $(40-80)$ GeV (top-left), $(80-120)$ GeV (top-right), $(120-160)$ GeV (bottom-left) and $(160-200)$ GeV (bottom-right).

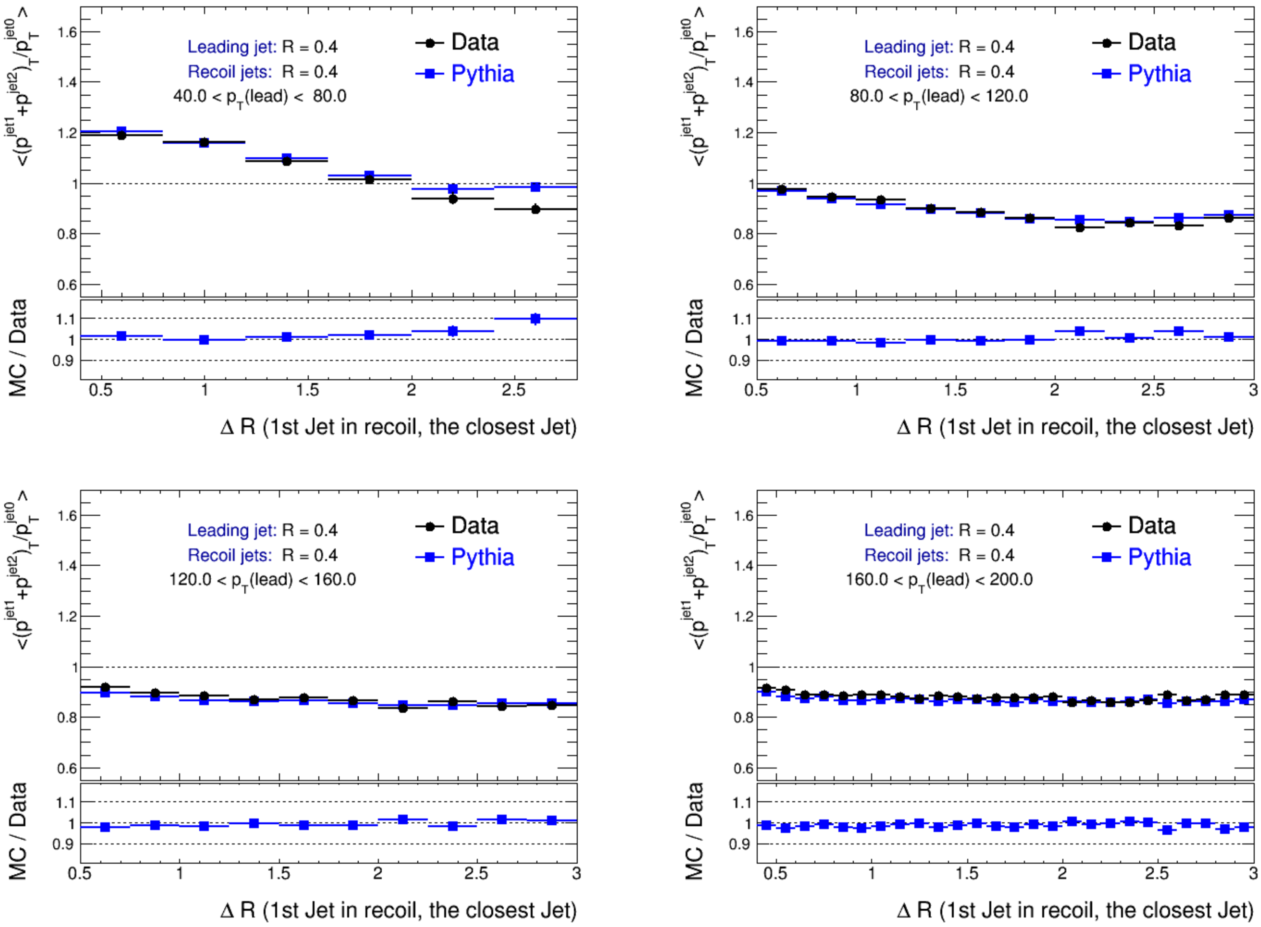

Figure 2.14: Comparison of response R spectra as a function of the ΔR and transverse momentum of leading jet $p_t(lead)$ for ATLAS data and MC Pythia 8. Response R values were reached by *individual fit procedure*. All spectra are associated with recoil system formed of $R = 0.4$ (Standard) jets. Response R is shown in four bins of $p_t(lead)$: $(40 - 80)$ GeV (top-left), $(80 - 120)$ GeV (top-right), $(120 - 160)$ GeV (bottom-left) and $(160 - 200)$ GeV (bottom-right).

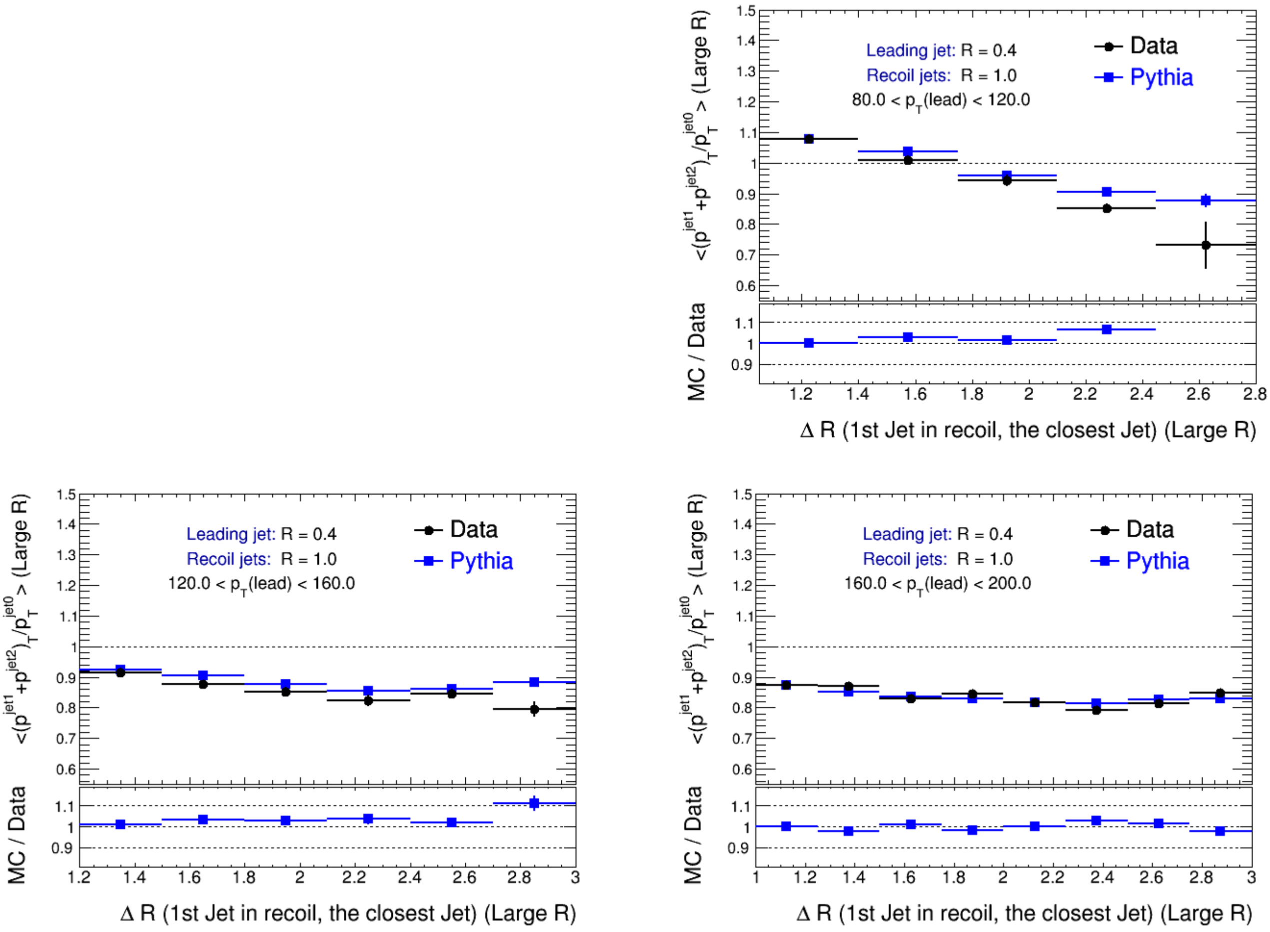

Figure 2.15: Comparison of response R spectra as a function of the ΔR and transverse momentum of leading jet $p_t(lead)$ for ATLAS data and MC Pythia 8. Response R values were reached by *individual fit procedure*. All spectra are associated with recoil system formed of $R = 1.0$ (Large) jets. Response R is shown in three bins of $p_t(lead)$: $(80 - 120)$ GeV (top-right), $(120 - 160)$ GeV (bottom-left) and $(160 - 200)$ GeV (bottom-right)

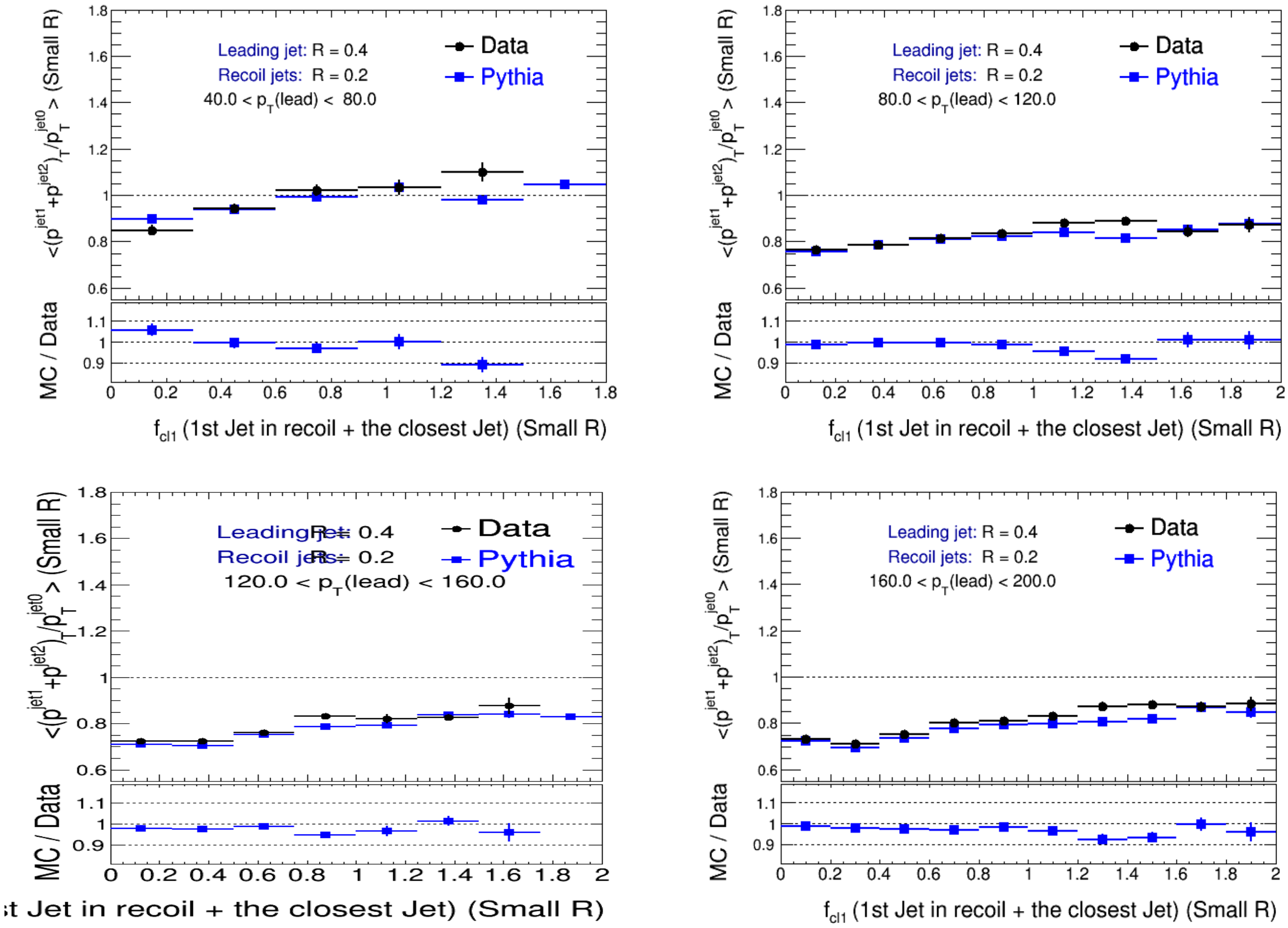

Figure 2.16: Comparison of response R spectra as a function of the f_{cl1} and transverse momentum of leading jet $p_t(lead)$ for ATLAS data and MC Pythia 8. Response R values were reached by *individual fit procedure*. All spectra are associated with recoil system formed of $R = 0.2$ (Small) jets. Response R is shown in four bins of $p_t(lead)$: $(40-80)$ GeV (top-left), $(80-120)$ GeV (top-right), $(120-160)$ GeV (bottom-left) and $(160-200)$ GeV (bottom-right)

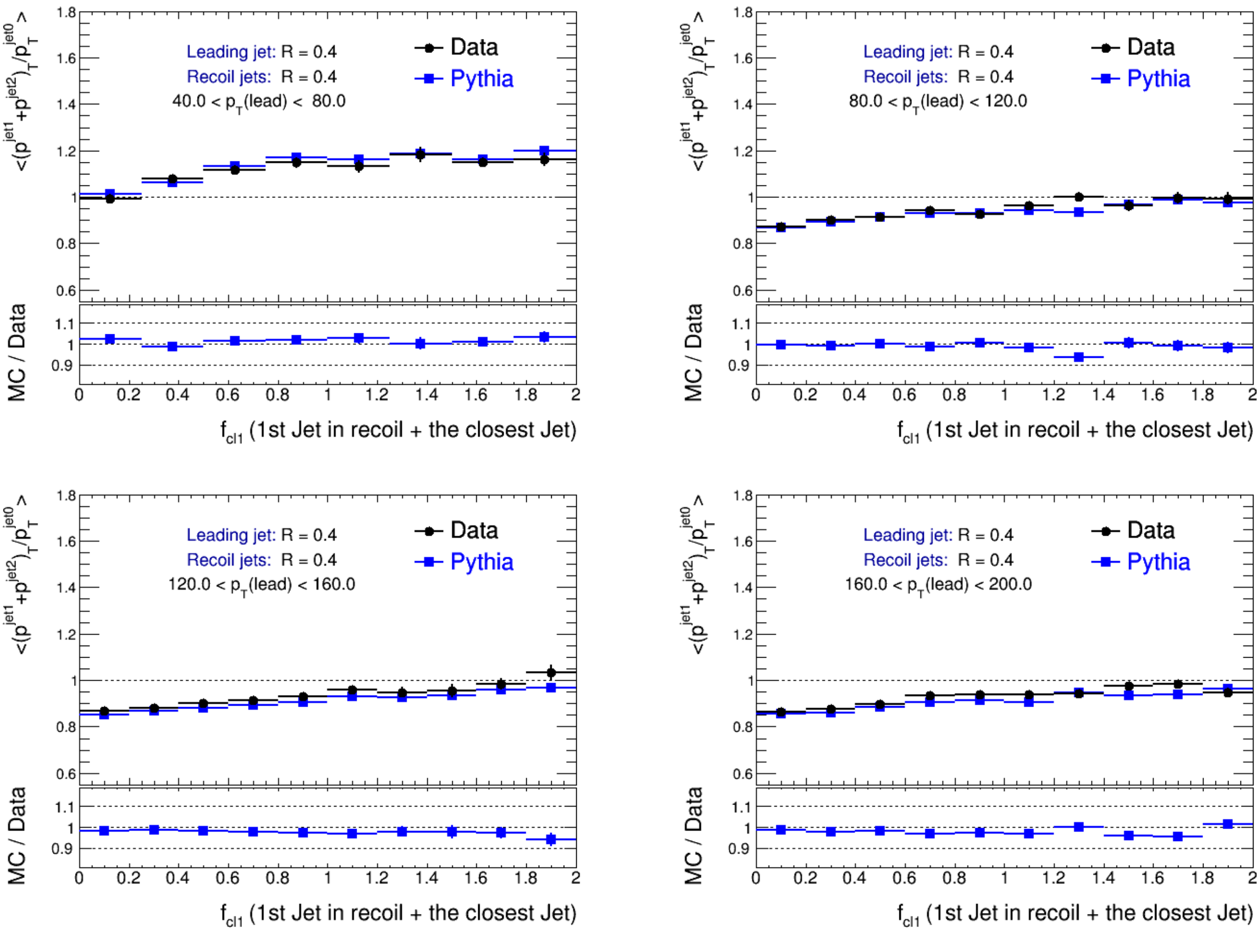

Figure 2.17: Comparison of response R spectra as a function of the f_{cl1} and transverse momentum of leading jet $p_t(lead)$ for ATLAS data and MC Pythia 8. Response R values were reached by *individual fit procedure*. All spectra are associated with recoil system formed of $R = 0.4$ (Standard) jets. Response R is shown in four bins of $p_t(lead)$: $(40-80)$ GeV (top-left), $(80-120)$ GeV (top-right), $(120-160)$ GeV (bottom-left) and $(160-200)$ GeV (bottom-right).

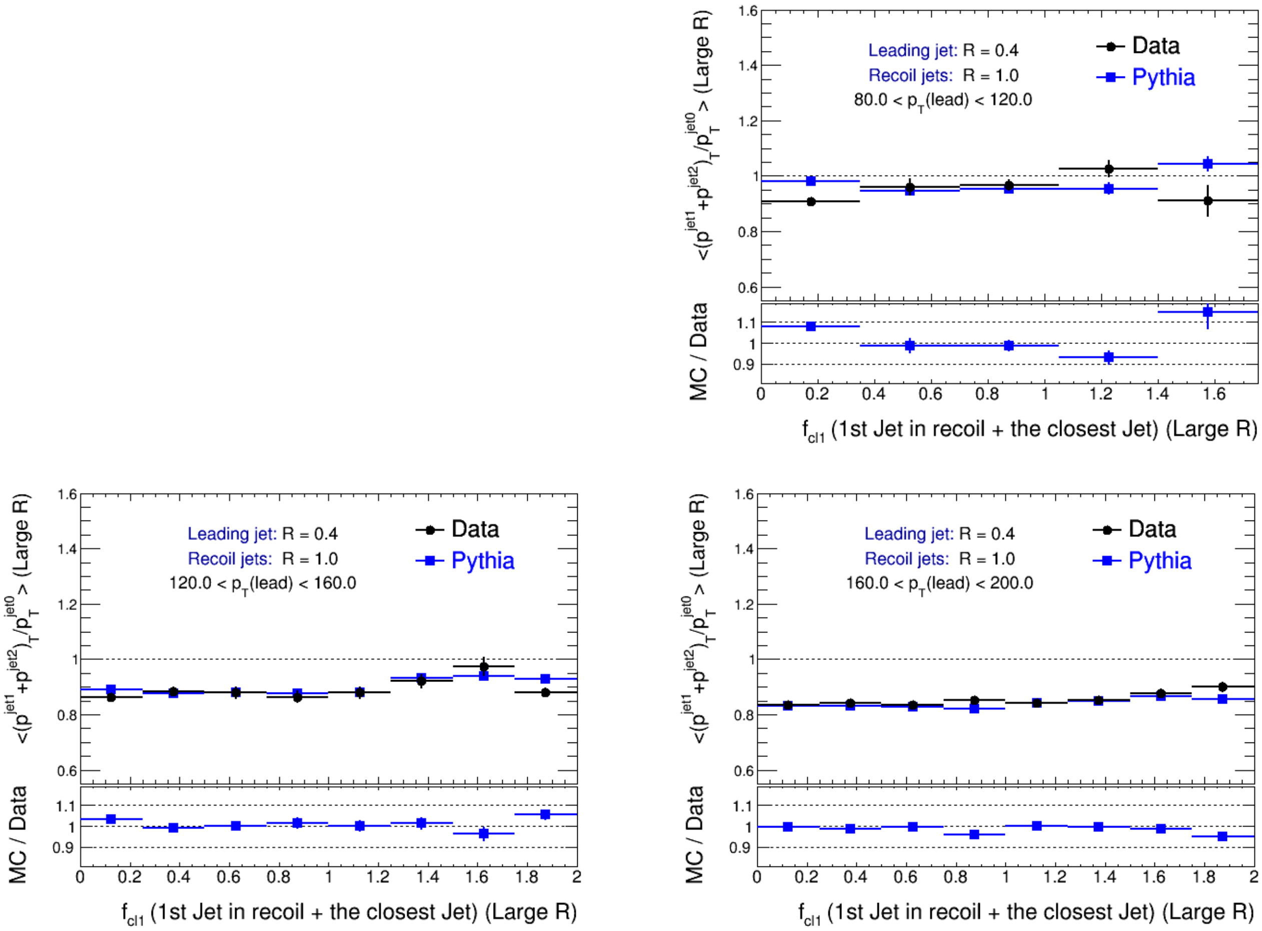

Figure 2.18: Comparison of response R spectra as a function of the $fcl1$ and transverse momentum of leading jet $p_t(lead)$ for ATLAS data and MC Pythia 8. Response R values were reached by *individual fit procedure*. All spectra are associated with recoil system formed of $R = 1.0$ (Large) jets. Response R is shown in three bins of $p_t(lead)$: $(80 - 120)$ GeV (top-right), $(120 - 160)$ GeV (bottom-left) and $(160 - 200)$ GeV (bottom-right).

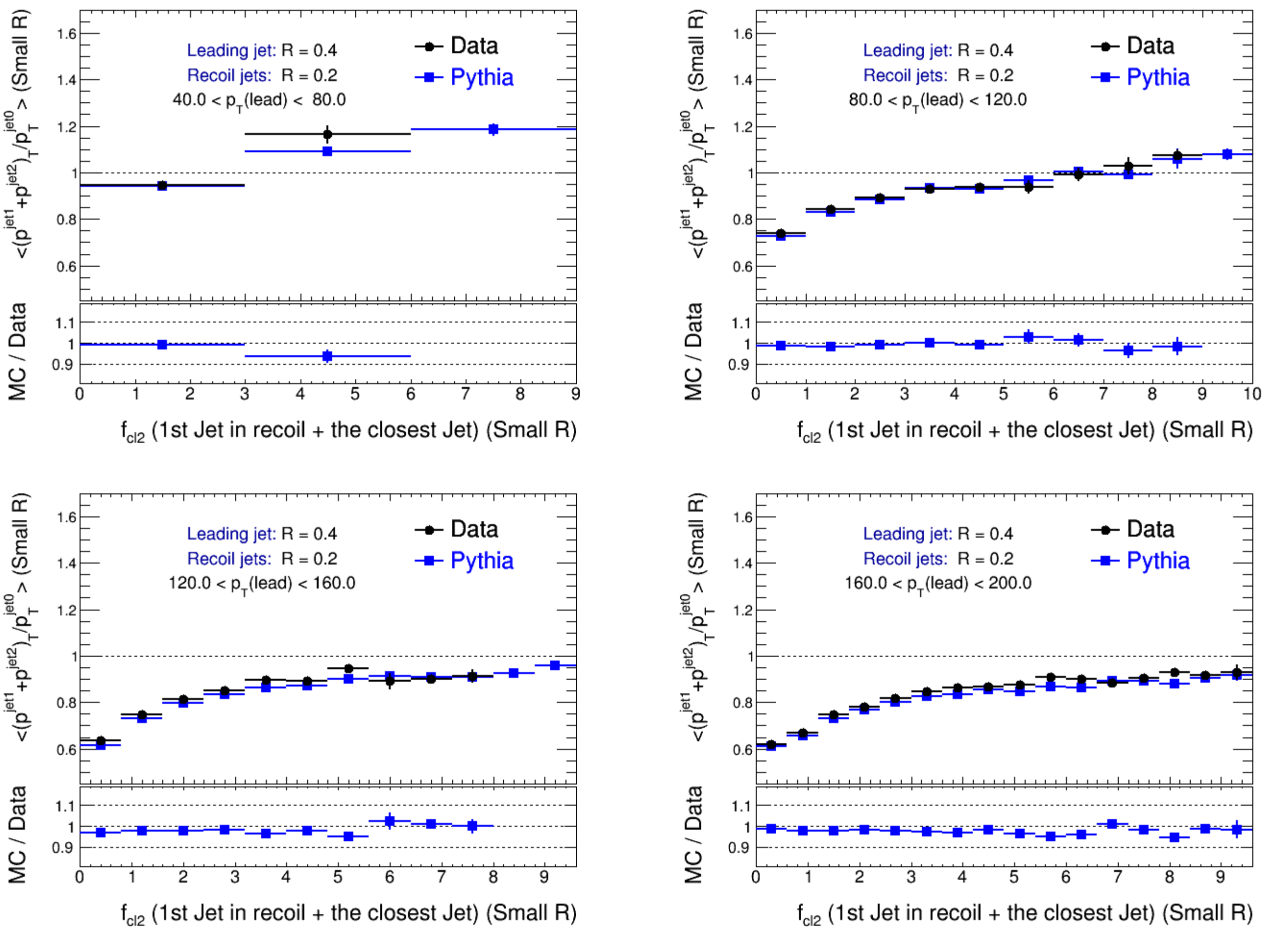

Figure 2.19: Comparison of response R spectra as a function of the f_{lc2} and transverse momentum of leading jet $p_t(lead)$ for ATLAS data and MC Pythia 8. Response R values were reached by *individual fit procedure*. All spectra are associated with recoil system formed of $R = 0.2$ (Small) jets. Response R is shown in four bins of $p_t(lead)$: $(40-80)$ GeV (top-left), $(80-120)$ GeV (top-right), $(120-160)$ GeV (bottom-left) and $(160-200)$ GeV (bottom-right).

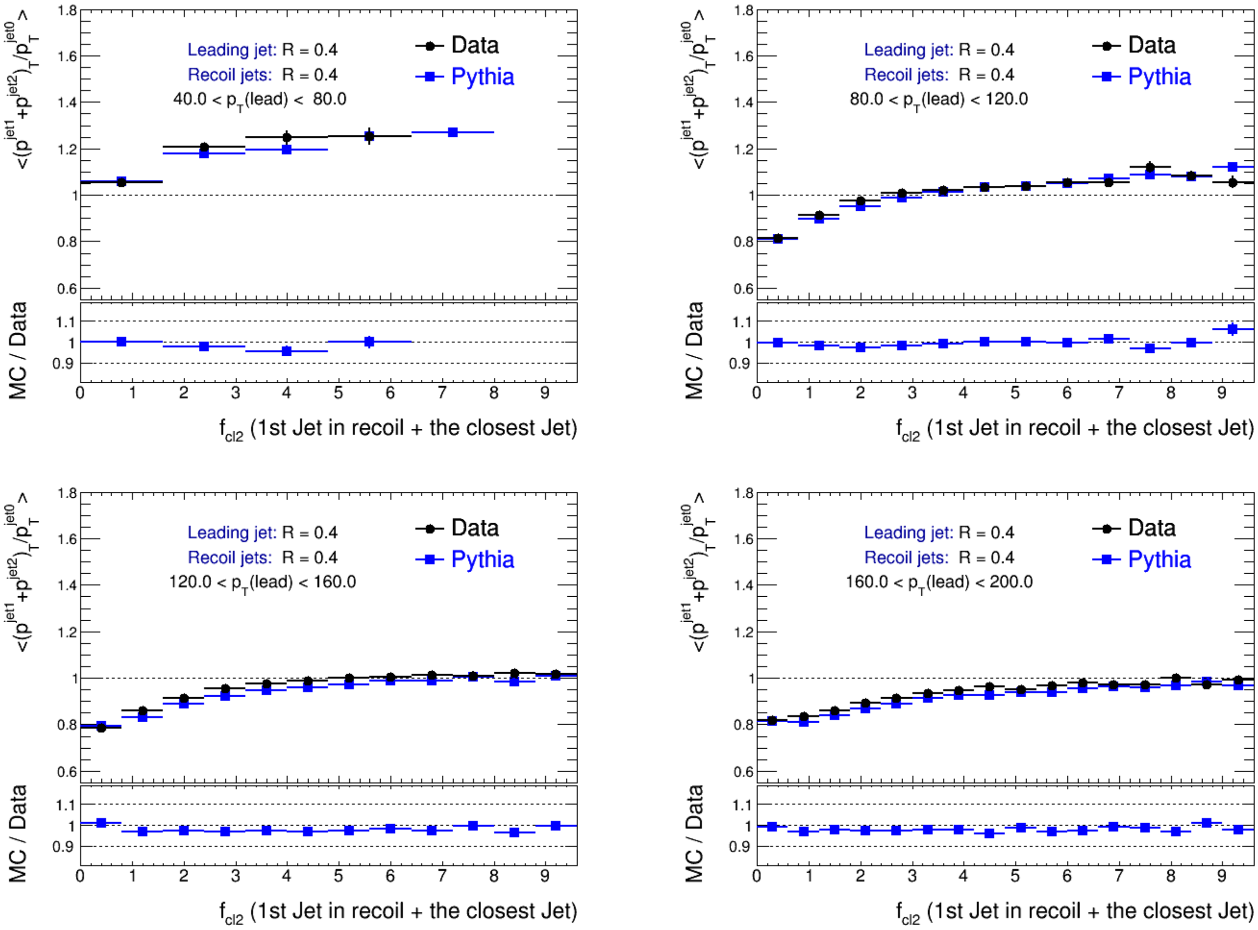

Figure 2.20: Comparison of response R spectra as a function of the f_{cl2} and transverse momentum of leading jet $p_t(lead)$ for ATLAS data and MC Pythia 8. Response R values were reached by *individual fit procedure*. All spectra are associated with recoil system formed of $R = 0.4$ (Standard) jets. Response R is shown in four bins of $p_t(lead)$: $(40 - 80)$ GeV (top-left), $(80 - 120)$ GeV (top-right), $(120 - 160)$ GeV (bottom-left) and $(160 - 200)$ GeV (bottom-right).

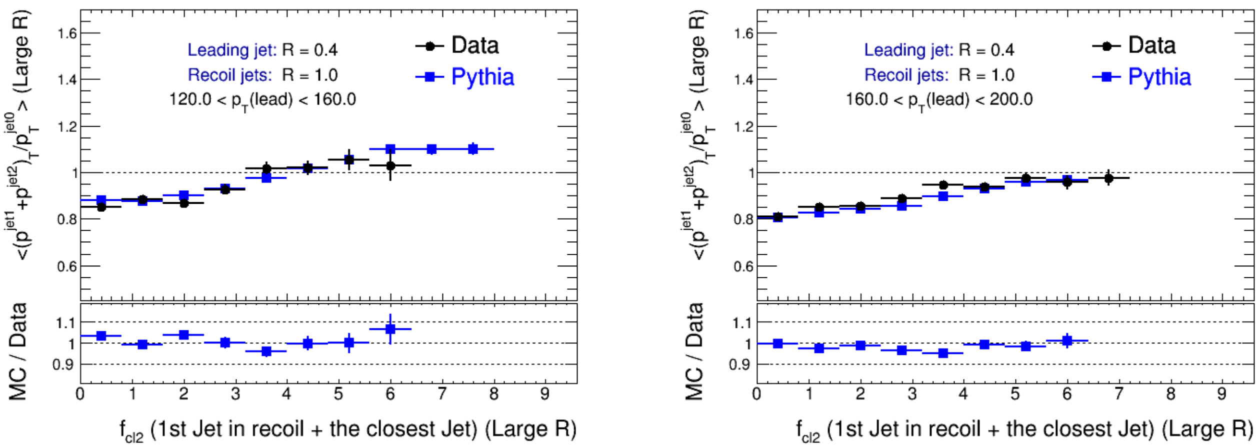

Figure 2.21: Comparison of response R spectra as a function of the f_{cl2} and transverse momentum of leading jet $p_t(lead)$ for ATLAS data and MC Pythia 8. Response R values were reached by *individual fit procedure*. All spectra are associated with recoil system formed of $R = 1.0$ (Large) jets. Response R is shown in four bins of $p_t(lead)$: $(120 - 160)$ GeV (left) and $(160 - 200)$ GeV (right).

Chapter 3

Conclusion

The thesis has two main parts. The first theoretical part describes the jets, jet's properties and the new techniques with emphasis on large R jets for new physics research. The second part represents the crucial section of the thesis. It corresponds to the analysis of close-by effects of jets.

Note, the computing centre Goliáš at Institute of Physics at Academy of Sciences of Czech Republic as well as LHC Word-Wide Grid were used for the data analysis.

The analysis study the jets with radii R = 0.2, 0.4 and 1.0 and two methods for their reconstruction: from calorimeter's clusters and from Small ($R = 0.2$) jets, which were further re-clustered. The analysis uses multijets event instead of the previous studies, which were based on well-balanced $dijet$ or $jet+boson$ systems. The close-by effects are mostly described by change of shape in spectra of response R variable as a function of various metrics distances (ΔR, f_{cl1} and f_{cl2}) in specific range of transverse momenta of leading jet $p_t(lead)$.

The computational part is divided into two parts with respect $p_t(lead)$. First first was focused on high-p_t scale (200 GeV$< p_t(lead) <$ 1000 GeV). In fact, it corresponds to analysis performed by R. Lysák and J. Hejbal. Their framework was used as a base for the second part focused on low-p_t scale. The task (study of close-by effects at low-p_t scale) was assigned by members of Jetsubstructure ATLAS group. This second part, low-p_t scale analysis, reaches the lowest $p_t(lead)$ as was possible (40 GeV$< p_t(lead) <$ 200 GeV).

The results of close-by effects at high-p_t scale are the following. The close-by effects were observed, but they are rather small (at $p_t(lead) >$ 200 GeV). The most sensitive variable for description of close-by effects was found to be f_{cl2} metric. The f_{cl2} variable does not consider only space resolution of two jets, but also their momenta. We observe the following trends: the significance of close-by effects increase with decreasing transverse momenta $p_t(lead)$. Further, the close-by effects are generally more visible for Small ($R = 0.2$) jets than Standard ($R = 0.4$). The ratio of ATLAS data and Pythia is quite good, mostly less than 5% level of disagreement. A general rule is that if the disagreement between data and MC is less than 2%, no other source of systematic uncertainty is needed to be added. Following this rule, we conclude that no systematic uncertainty is connected to the close-by effects for $p_t(lead) >$ 600 GeV, while for $p_t(lead) <$ 600 GeV, the disagreement reaches up to 5%, so this source should be considered in the total jet energy scale uncertainty. Further, any close-by effects are not seen for Large R jets at $p_t(lead) >$ 400 GeV, therefore it seem, that Small ($R = 0.2$) jets could be used for re-clustering Large R ($R = 1.0$) jets safely from $p_t(lead) >$ 400 GeV. The results of this part are found to be in a very good agreement with those presented in the ATLAS Note [10].

The close-by effects were observed at low-p_t analysis, too. The results verify that the close-by effects become more significant with increasing $p_t(lead)$. However, the close-by effects of Small ($R = 0.2$) and Standard ($R = 0.4$) jets appear comparable at $40 - 120$ GeV of $p_t(lead)$ for all studied metrics. It could consider with insufficient balance of studied system at $p_t(lead) <$ 120 GeV. The insuffition balance is caused by p_t selection criteria. Therefore the results are only orientative at $p_t(lead) <$ 120 GeV. Further, Large R jets were not almost reconstructed at $p_t(lead) <$ 120 GeV. The buiding Large R jets from Small ($R = 0.2$) jets using re-clustering is not clearly safety, the close-by effects are still well observed at f_{cl2} distributions at $p_t(lead) < 200$ GeV. The data are still well described by MC Pytiha 8, the level of disagreement is less than 6% of disagreement, except the last problematic bins in shown spectra. All in all the results are not still enough precise to confirme another energy scale systematic uncertiecty due close-by effects of jets. For jets with p_t smaller than 200 GeV, we observe roughly the same tendencies as for the high-p_t jets but they are much more pronounced. So consistently with observation made in the high-p_t analysis, the re-clustering of Large R jets from Small R jets is not recommended for jets with $p_t < 200$ GeV but a safer threshold lies already at the value around 400 GeV. Similarly as in the high-p_t analysis, the most sensitive variable found to study the close-by effects is f_{cl2}.

Chapter 4

Back-up

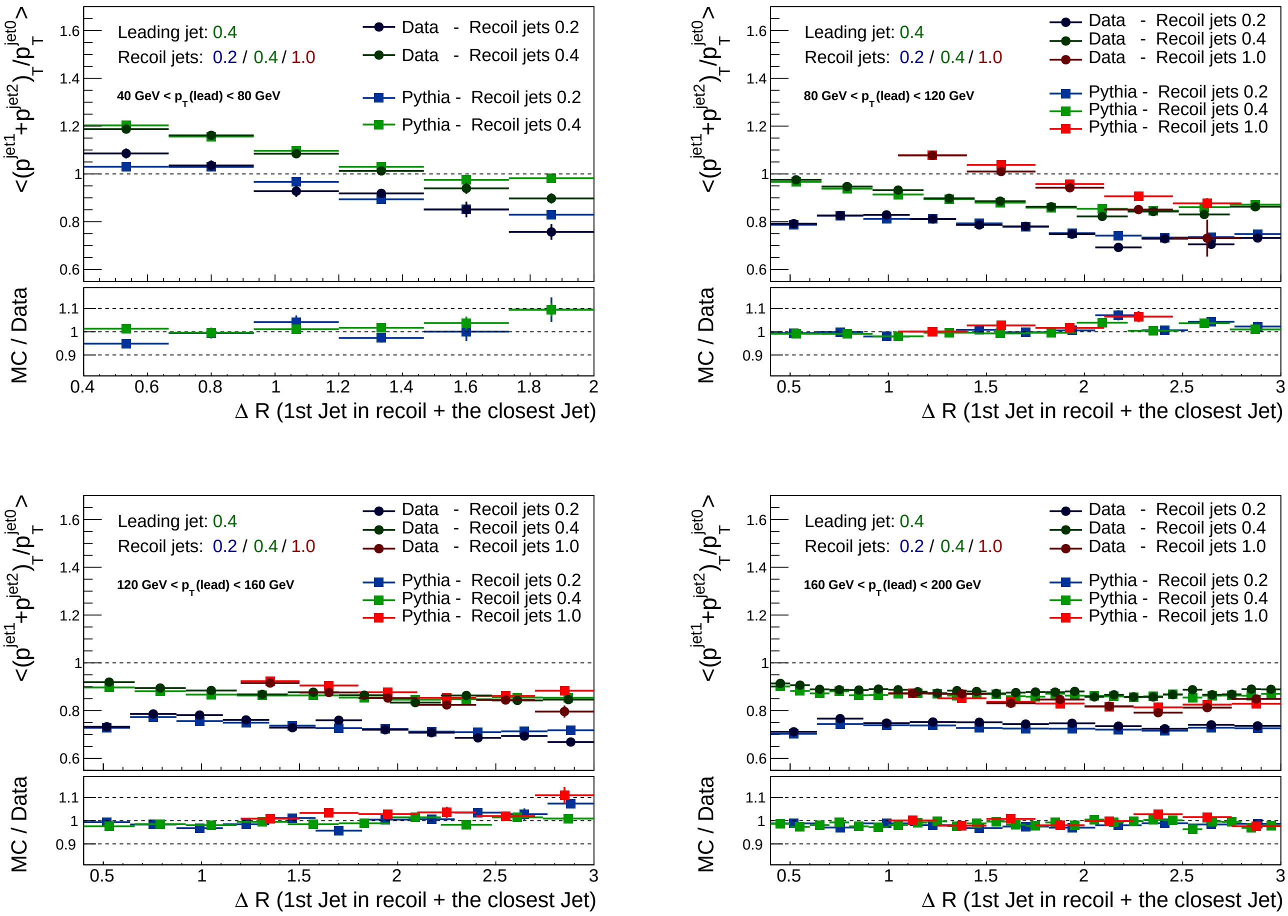

Figure 4.1: Comparison of response R spectra using as a function of the ΔR and transverse momentum of leading jet $p_t(lead)$ for ATLAS data and MC Pythia 8. Response R values were reached by *individual fit procedure*. The dependencies are shown for various radii $R = 0.2/0.4/1.0$ of recoil jets, therefore slighly differences of close-by effects (for different R jets) are visible. Response R is shown in four bins of $p_t(lead)$: $(40-80)$ GeV (top-left), $(80-120)$ GeV (top-right), $(120-160)$ GeV (bottom-left) and $(160-200)$ GeV (bottom-right)

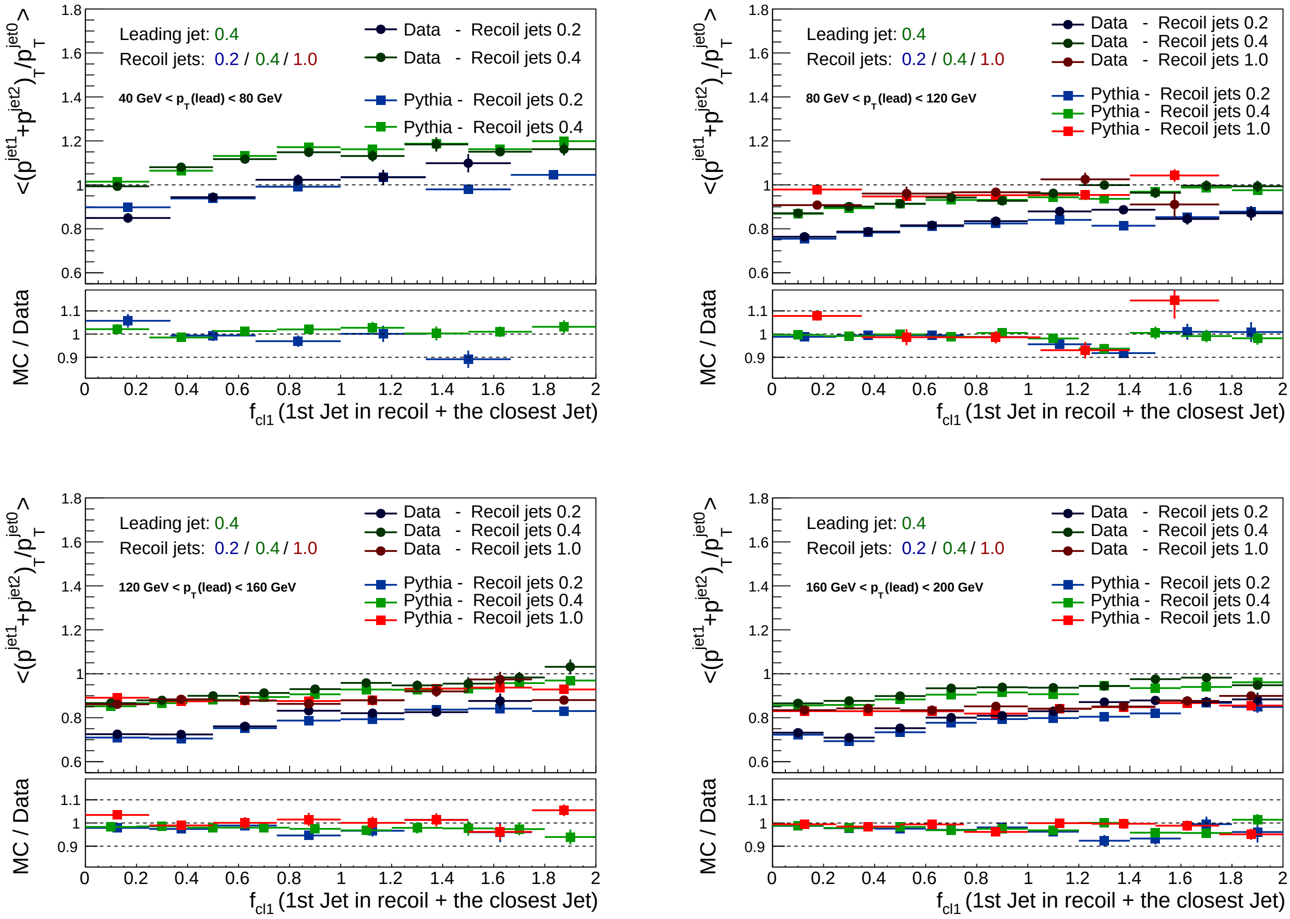

Figure 4.2: Comparison of response R spectra using as a function of the f_{cl1} and transverse momentum of leading jet $p_t(lead)$ for ATLAS data and MC Pythia 8. Response R values were reached by *individual fit procedure*. The dependencies are shown for various radii $R = 0.2/0.4/1.0$ of recoil jets, therefore slighly differences of close-by effects (for different R jets) are visible. Response R is shown in four bins of $p_t(lead)$: $(40-80)$ GeV (top-left), $(80-120)$ GeV (top-right), $(120-160)$ GeV (bottom-left) and $(160-200)$ GeV (bottom-right)

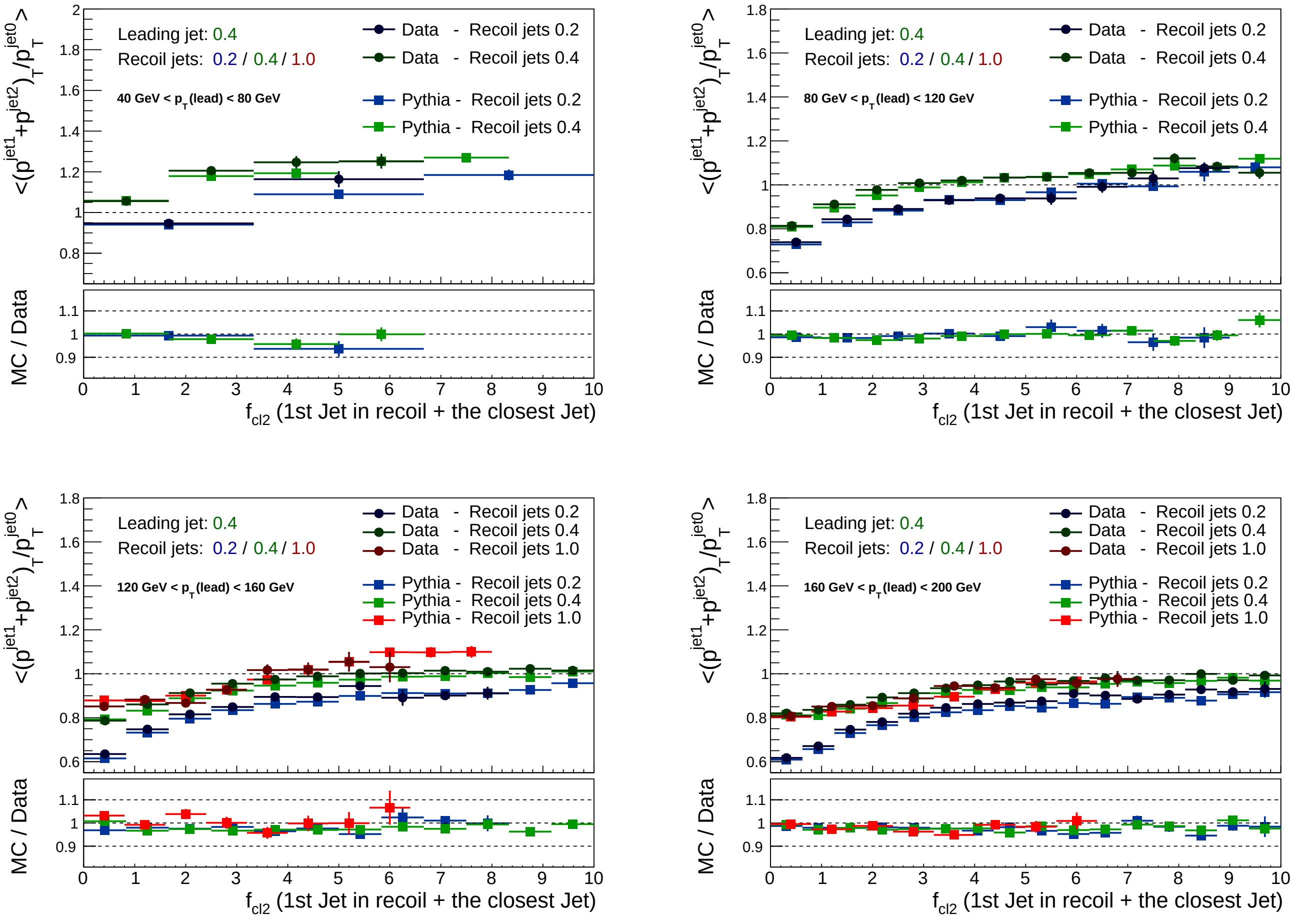

Figure 4.3: Comparison of response R spectra using as a function of the f_{cl2} and transverse momentum of leading jet $p_t(lead)$ for ATLAS data and MC Pythia 8. Response R values were reached by *individual fit procedure*. The dependencies are shown for various radii $R = 0.2/0.4/1.0$ of recoil jets, therefore slighly differences of close-by effects (for different R jets) are visible. Response R is shown in four bins of $p_t(lead)$: $(40-80)$ GeV (top-left), $(80-120)$ GeV (top-right), $(120-160)$ GeV (bottom-left) and $(160-200)$ GeV (bottom-right)

Bibliography

[1] M. Cacciari and G. P. Salam, *"Pileup subtraction using jet areas"*, *Phys. Lett.* **B 659** (2008) 119–126 arXiv:0707.1378 [hep-ph].

[2] ATLAS Collaboration, *"Performance of jet substructure techniques for large-R jets in proton-proton collisions at $\sqrt{s} = 7$ TeV using the ATLAS detector"*, arXiv:1306.4945v [hep-ex]

[3] M. Cacciari, G. P. Salam, *"The anti-k t jet clustering algorithm"*, arXiv:0802.1189v2 [hep-ph]

[4] G. P. Salam, *"Towards Jetography"*, arXiv:0906.1833v2 [hep-ph]

[5] ATLAS Collaboration, *"Jet Re-clustering in ATLAS"*, tech. rep. ATL-COM-PHYS-2014-1117, CERN, 2014

[6] J. Heinrich, *"Reconstruction of boosted $W^{\pm}$ and Z^{0} bosons from fat jets"*, tech. rep. CERN-THESIS-2014-152, CERN, 2014

[7] ATLAS Collaboration, *"Search for dark matter in events with a hadronically decaying W or Z boson and missing transverse momentum in pp collisions at $\sqrt{(s)} = 8$ TeV with the ATLAS detector"*, Phys. Rev. Lett 112 (2014) 041802, tech. rep. arXiv:1309.4017 [hep-ex], CERN, 2014

[8] J. M. Butterworth et al., *"Jet substructure as a new Higgs search channel at the LHC"*, Phys. Rev. Lett. 100 (2008) 242001, arXiv:0802.2470 [hep-ph], 2008

[9] B. Cooper, P. Starovoitov and F. Vives, *"Studies of Jet Energy Scale Uncertainties due to Close-By Effects in $\sqrt{s} = 8$ TeV Data"*, tech. rep. ATL-COM-PHYS-2013-983, CERN, 2013

[10] J. Hejbal, R. Lysak, *"Close-by jets studies in multijet events"*, tech. rep. ATL-COM-PHYS-2017-067, CERN, 2017

[11] MultijetBalance package svn location: `//svn.cern.ch/reps/atlasperf/436CombPerf/JetETMiss/Run2/Jet/Calibration/JetCalibrationTools/InSitu/437MultijetBalance/MultijetBalanceAlgo/tags/MultijetBalanceAlgo-00-00-02`

[12] xAODAnalHelper package svn location: `//svn+ssh://svn.cern.ch/reps/atlasinst/439Institutes/UChicago/xAODAnaHelpers/tags/xAODAnaHelpers-00-03-32`